IRONLESS ARMATURE TORQUE MOTOR

(Contract No.: NAS-5-11481)

R. L. Fisher
Brushless D. C. Motors
Sperry Marine Systems Division
Sperry Rand Corporation
Charlottesville, Virginia 22901

September 10, 1972
Final Report for Period July 1971 - July 1972
Report No. JA 700-0020

Prepared for

GODDARD SPACE FLIGHT CENTER
Greenbelt, Maryland 20771

1. Report No.	2. Government Accession No.	3. Recipient's Catalog No.
JA 700-0020		

4. Title and Subtitle	5. Report Date
IRONLESS ARMATURE TORQUE MOTOR	September 10, 1972
	6. Performing Organization Code

7. Author(s)	8. Performing Organization Report No.
R. L. Fisher	

9. Performing Organization Name and Address	10. Work Unit No.
Brushless DC Motors Sperry Marine Systems Division Sperry Rand Corporation Charlottesville, Virginia 22901	11. Contract or Grant No. NAS 5-11481
12. Sponsoring Agency Name and Address P. A. Studer, Code 721 Goddard Space Flight Center Greenbelt, Maryland 20771	13. Type of Report and Period Covered Final Report for period July 1971 - July 1972
	14. Sponsoring Agency Code

15. Supplementary Notes

16. Abstract

This report provides a record of the work performed on NASA contract NAS 5-11481. The contract involved the development and manufacture of a low-speed ironless armature torque motor (less electronics). Four ironless armature torque motors, four Hall device position sensor assemblies, and two test fixtures were fabricated.

The design approach utilized samarium cobalt permanent magnets, a large airgap, and a three-phase winding in a stationary ironless armature. Hall devices were employed to sense rotor position.

An ironless armature torque motor having an outer diameter of 4.25 inches was developed to produce a torque constant of 65 ounce-inches per ampere with a resistance of 20.5 ohms. The total weight, including structural elements, was 1.58 pounds.

Test results indicated that all specifications were met except for generated voltage waveform. It is recommended that investigations be made concerning the generated voltage waveform to determine if it may be improved.

17. Key Words (Selected by Author(s))	18. Distribution Statement
Development of a Low-Speed Ironless Armature Torque Motor	

19. Security Classif. (of this report)	20. Security Classif. (of this page)	21. No. of Pages	22. Price*
Unclassified	Unclassified	58	5.00

*For sale by the Clearinghouse for Federal Scientific and Technical Information, Springfield, Virginia 22151.

PREFACE

This report provides a record of the work performed on NASA contract NAS 5-11481. The contract involved the development and manufacture of a low-speed ironless armature torque motor (less electronics). Four ironless armature torque motors, four Hall device position sensor assemblies, and two test fixtures were fabricated.

The design approach utilized samarium cobalt permanent magnets, a large airgap, and a three-phase winding in a stationary ironless armature. Hall devices were employed to sense rotor position.

An ironless armature torque motor having an outer diameter of 4.25 inches was developed to produce a torque constant of 65 ounce-inches per ampere with a resistance of 20.5 ohms. The total weight, including structural elements, was 1.58 pounds.

Test results indicated that all specifications were met except for generated voltage waveform. It is recommended that investigations be made concerning the generated voltage waveform to determine if it may be improved.

TABLE OF CONTENTS

LIST OF ILLUSTRATIONS

LIST OF ILLUSTRATIONS (Cont)

LIST OF TABLES

SECTION I

INTRODUCTION

The following report describes the results of the work performed on contract NAS 5-11481 for the development and manufacture of a low-speed ironless armature torque motor (less electronics).

This contract involved the design and fabrication of a permanent magnet field assembly, a wound, shell-type armature for three-phase operation with the above permanent magnet assembly, Hall effect devices to provide angular position signals proportional to the magnetic field, and structural elements to integrate the magnet field assemblies into a testable device. Four ironless armature torque motors, four Hall device position sensor assemblies, and two test fixtures were fabricated.

Because of the unique design of this torque motor, there are no breakaway, cogging, or magnetic friction torques. The electrical time constant is very low. Static decentering forces are eliminated. Heat can be readily conducted away from the stationary winding assembly.

Due to the elimination of friction torque, this motor lends itself to applications in precision position servos and momentum wheels. The electrical time constant is approximately one-tenth of the time constant of the conventional torque motor thus making possible high speed operation. The elimination of decentering forces offers a tremendous advantage when mounting motors on electromagnetic bearings.

SECTION II

OPERATING CHARACTERISTICS

The specifications for the development of an ironless armature torque motor per specification No. S-721-P-4 are listed in Table 2-1 and compared with tested values obtained from the first engineering model. All specifications were met or exceeded except for generated voltage waveform and weight.

TABLE 2-1. PERFORMANCE CHARACTERISITCS

PARAMETER	DESIGN REQUIREMENTS	TEST VALUE (First Engineering Model)
Torque Sensitivity	40 oz-in. /amp minimum	65 oz-in. /amp
Armature Resistance (Delta)	20 ohms maximum	16.3 ohms
Weight (Wire, Magnetic Parts)	1.0 lb maximum	1.07 lb
Outside Diameter (OD)	4.25" maximum	4.25" maximum
Inside Diameter (ID)	2.25" minimum	2.25" minimum
Sensor Output	4 mv/ma ±100 mv at 120°E	±650 mv at 120°E

The design was modified to provide for Hall effect devices external to the armature assembly and for increased mechanical gaps between the armature assembly and the rotor assembly. The position of the Hall device assembly was made adjustable for optimizing the commutation angle. Hall devices were mounted so as to provide a sinusoidal output. The zero crossover point was to be used to provide commutation information. The final performance specifications are shown in Table 2-2. The outline dimensions are shown in Figure 2-1.

TABLE 2-2. IRONLESS ARMATURE TORQUER SPECIFICATIONS

MOTOR SPECIFICATIONS:	VALUES
Torque constant (3-phase delta)	65 oz-in. /amp
Back emf constant (peak)	0.5 volts/rad/sec
DC resistance per phase	30.8 ohms
DC Resistance (delta)	20.5 ohms
Inductance (delta)	4.1×10^{-3} Henrys
Electrical time constant (L/R)	0.2×10^{-3} sec
Weight (including structure elements)	1.58 lb
Motor friction torque	0
Motor constant (oz-in. /amp/ $\sqrt{\text{ohm}}$	14.4
Number of poles	12
Outside diameter	4.249 +0.000 in. -0.002 in.
Inside diameter	2.6250 +0.0000 in. -0.0002 in.
HALL DEVICE SENSOR ASSEMBLY:	
Type Hall device	Siemens SV 110-II
Input current (green leads)	10 milliamperes
Cycles per revolutation	6
Number of Hall devices	3 Hall devices 120 elec degrees apart

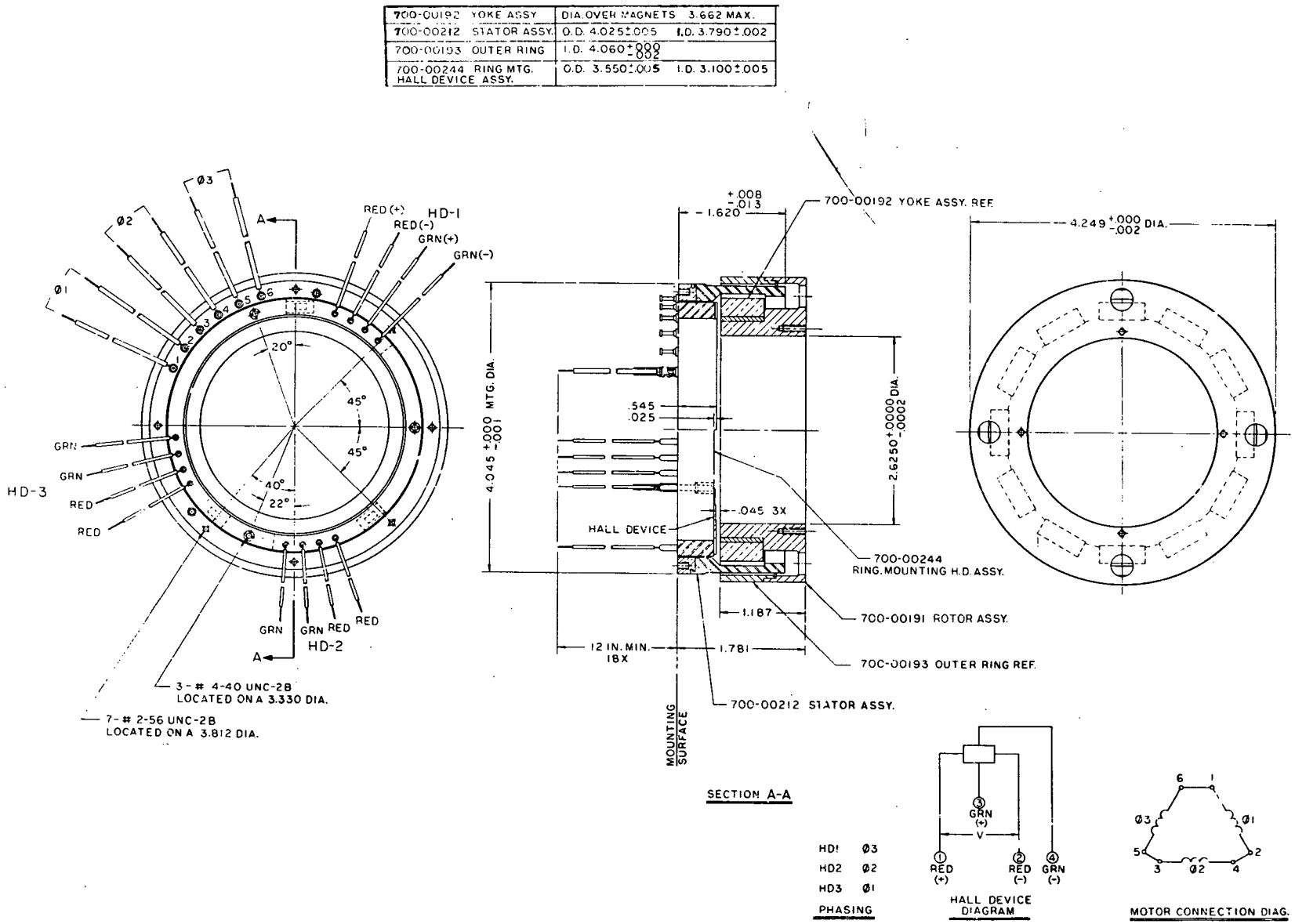

Figure 2-1. Ironless Armature Torque Motor, Outline Drawing

SECTION III

TECHNICAL APPROACH

GENERAL DESCRIPTION

The ironless armature torque motor is similar in construction to a printed circuit motor. However, the permanent magnet field rotates instead of the printed circuit armature. The stator assembly contains the windings and is attached to an aluminum mounting ring on one end. The stator is positioned in a radial gap. The winding assembly, having no magnetic materials, effects the elimination of magnetic losses.

MAGNETIC DESIGN

The magnetic design for an ironless armature torque motor requires a design that is capable of driving as much magnetic flux as possible across a large airgap. In addition, a very accurately shaped magnetic field is necessary to obtain the desired generated voltage and sensor output waveforms (see Figure 3-1 and Figure 3-2). A square wave magnetic field having a width of 120 electrical degrees is desired. For meeting these requirements, a magnet material having a very high coercive force and capable of high flux density was required. Therefore, samarium cobalt permanent magnets, which have the highest available energy product, were used. The properties of samarium cobalt are shown in Table 3-1. Samarium cobalt has the added advantages of being both an extremely stable material, with practically no long-term variation, and a highly oriented material, which minimizes leakage fields.

The next magnetic consideration was to determine the number of poles. A high number of poles requires tighter tolerances on magnet position, magnet pole span, coil position, and on the position of the Hall device sensors. However, with fewer poles, the back iron for closing the magnetic circuits is thicker. This increases the weight and shortens the possible magnet length. The mean length of turn for the conductors is thereby increased, thus increasing the resistance.

Four rectangular samarium cobalt permanent magnets, with the dimensions 22.9 mm x 10.2 mm x 6.4 mm (0.9 in. x 0.4 in. x 0.25 in.), were purchased from the Raytheon Company. The direction of magnetism was along the 6.4 mm dimension. Also, two sample cylindrical samarium cobalt magnets, with the dimensions 12.7 mm (0.5 in.) diameter by 5 mm (0.2 in.) length, were obtained from the Electron Energy Corporation.

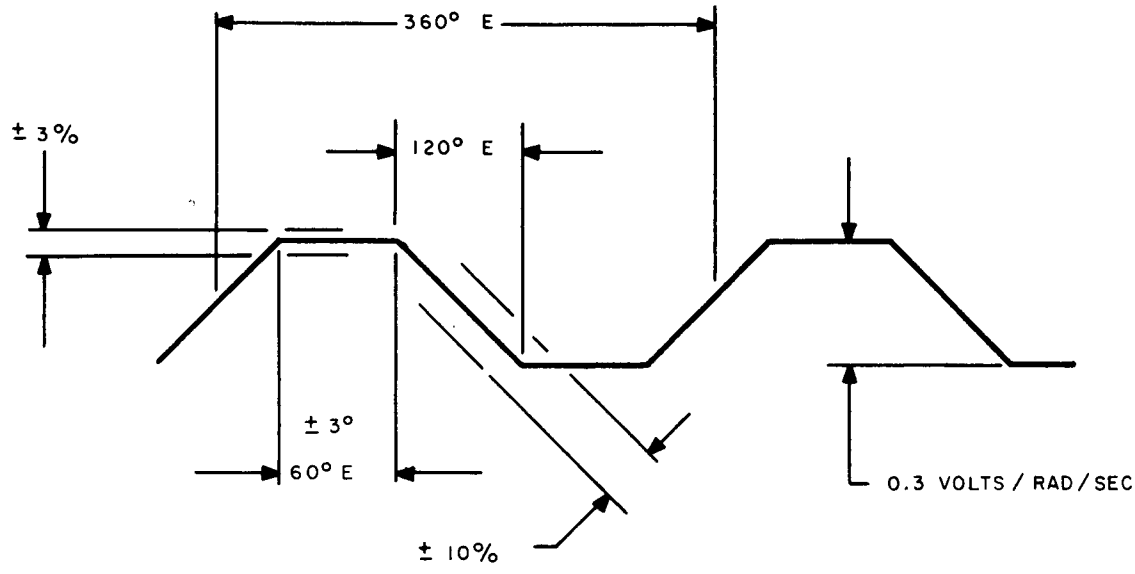

Figure 3-1. Generated Voltage Waveform,
Each of 3 Coils, Displaced 120°E

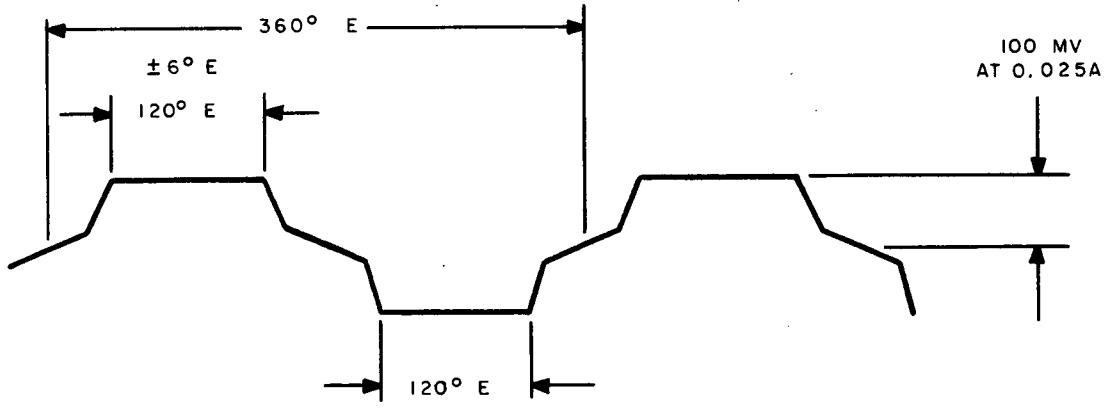

Figure 3-2. Sensor Output Waveform,
Each of 3 Hall Sensors, Displaced 120°E

TABLE 3-1. PROPERTIES OF SAMARIUM COBALT PERMANENT MAGNET

MAGNETIC PROPERTIES	
Residual Induction, B_r, Gauss	8,200
Coercive Force, H_c, Oe	7,800
Intrinsic Coercive Force, H_{ci}, Oe	>20,000
Maximum Energy Product, $(B_dH_d)m$, GOe	15×10^6
Intrinsic Energy Product, $(4\pi M \times H)_m$, GOe	80×10^6
Reversible Temperature Coefficient, %/°C	0.023
Average Recoil Permeability (slope of demagnetizing curve) for B/H 0.2	1.1
Curie Temperature, °C	750
PHYSICAL PROPERTIES	
Density, g/cc	8.3
Open Porosity, %	0
Tensile Strength, psi	8,000
Flexural Strength, psi	12,000
Hardness, Rockwell C	55
Thermal Expansion Coefficient, in./in./°C	10×10^{-6}
Thermal Conductivity, cgs	0.02
Electrical Resistivity, ohm-cm	5×10^{-4}

The rectangular magnets were assembled as shown in Figure 3-3. The flux density in the airgap was measured with a Hall probe and gaussmeter. The back iron for the magnet assembly was constructed so that both the airgap (G) and the magnet spacing (Y) could be varied. The airgap flux density was plotted first with magnets on one side of the airgap and then with magnets on both.

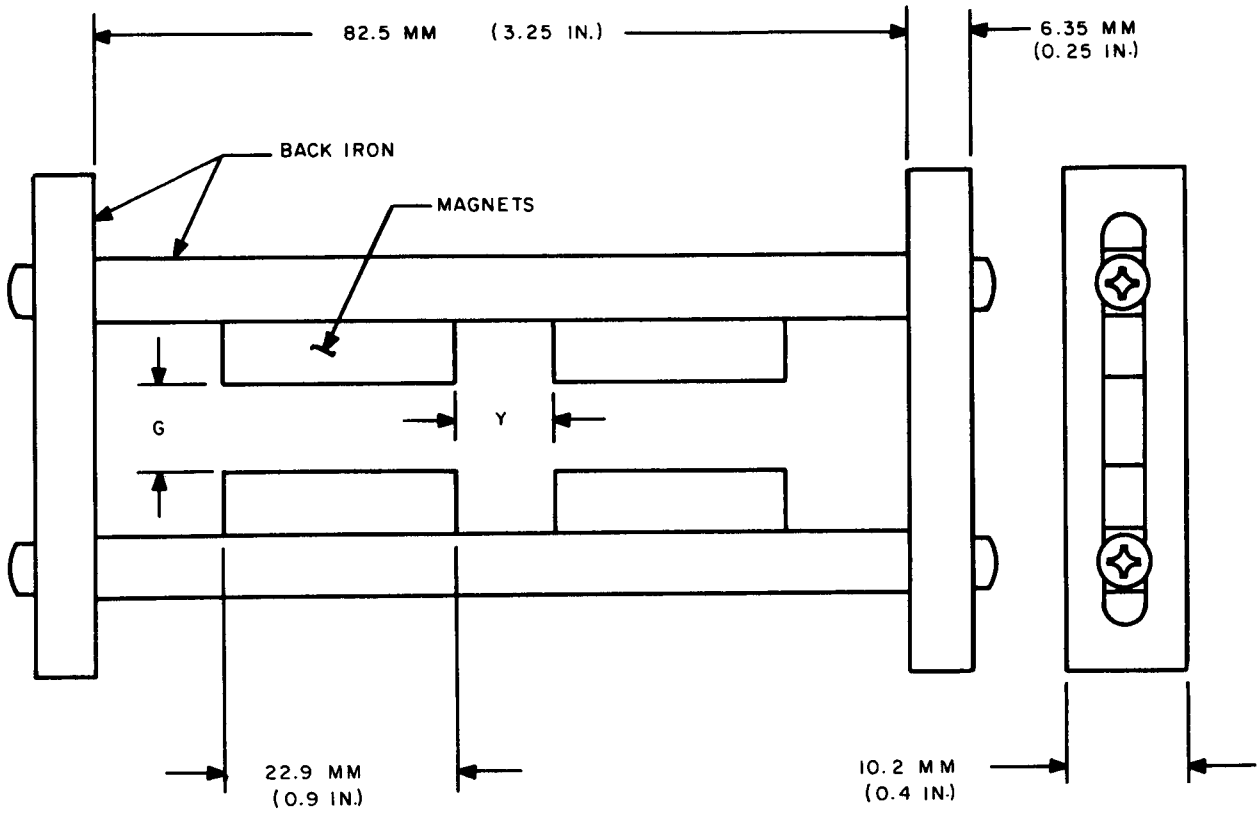

Figure 3-3. Magnet Assembly

Using these two magnet configurations, the following conclusions were drawn from data concerning the flux density magnitude and flux distribution:

1. The measured flux density in the airgaps at the center of the magnets with a 5 mm (0.2 in.) airgap was in agreement with calculated values. However, due to leakage, the flux density decreased as the Hall probe was moved toward the magnet edges. This resulted in lower flux per pole than figured in preliminary calculations.

2. Due to the leakage flux, the proposed square wave flux distribution did not exist. The corners of the waveshape were rounded. With this flux waveshape, it was felt that accurate switch points from the Hall device outputs would not be possible. However, Hall devices could still be used in the airgap to detect the zero crossover point and this information used for commutation switching.

3. Evaluation of the magnet spacing indicated that the best generated voltage waveform occurred when the distance between the magnets was equal to one-half the magnet width (120-degree pole span) as originally proposed.

4. The motor constant (oz-in./amp/$\sqrt{R}$) versus airgap was calculated for the two configurations. An airgap of 5.85 mm (0.230 in.) gave the maximum motor constant for the configuration having magnets on both sides of the airgap. An airgap of 5 mm (0.200 in.) was found to be optimum for the magnet configuration having magnets on only one side.

5. Using various numbers of poles, calculations were made to determine the motor constant and weight for the two configurations (see Table 3-2). The single magnet configuration was found to have less weight for a given motor constant for fourteen or more poles.

6. The single magnet configuration was choosen for this design. Not only is this configuration cheaper to manufacture, but also magnet cost is reduced due to the smaller number of magnets required.

TABLE 3-2. CALCULATIONS FOR MOTOR CONSTANT AND WEIGHT

No. of Poles	Single Magnet Configurations				
	Motor Constant (oz-in./amp/$\sqrt{R}$)	Weight (lb)			
		Iron	Wire	Magnets	Total
14	9.17	0.29	0.30	0.31	0.90
16	9.52	0.25	0.28	0.31	0.84
20	10.22	0.21	0.24	0.31	0.76
22	10.49	0.19	0.23	0.31	0.73

No. of Poles	Double Magnet Configurations				
	Motor Constant (oz-in./amp/$\sqrt{R}$)	Weight (lb)			
		Iron	Wire	Magnets	Total
14	9.27	0.24	0.20	0.48	0.92
16	9.69	0.21	0.19	0.48	0.88
20	10.35	0.17	0.16	0.48	0.81
22	10.60	0.16	0.15	0.48	0.79

In selecting the number of poles for the motor, the objective was to obtain the best generated waveform possible and meet the required weight of one pound. The weight specification was interpreted to mean the weight of the iron, magnets, and wire only. On this basis, twelve poles, with a calculated weight of 1.05 pounds, were chosen.

Motor Design

Using the required motor dimensions and the airgap dimensions obtained from the previous studies, the final design was calculated.

OD	=	Outside diameter = 4.25 in. max.
ID	=	Inside diameter = 2.25 in. max.
M_w	=	Axial length of magnet assembly = 0.60 in.
g	=	Airgap = 0.200 in.
Outer ring ID	=	4.060 in.

The operating point of the magnets (B_m/H_m) was calculated first.

$$\frac{B_m}{H_m} = \frac{A_g\, l_m}{H_m\, l_g}$$

$$= \frac{(0.406 \text{ in.}^2)\,(0.250 \text{ in.})}{(0.387 \text{ in.}^2)\,(0.200 \text{ in.})}$$

$$= 1.31$$

where

B_m	=	Flux density of magnet	
H_m	=	Field density of magnet	
A_g	=	Airgap area = 0.406 in.^{2}	(261.9 mm^2)
A_m	=	Magnet area = 0.387 in.^{2}	(249.7 mm^2)
l_g	=	Airgap length = 0.200 in.	(5.08 mm)
l_m	=	Magnet length = 0.250 in.	(6.35 mm)

From the magnet curve the induction at a B_m/H_m of 1.31 is 4.5 kilogauss or 29 kilolines per square inch (see Figure 3-4).

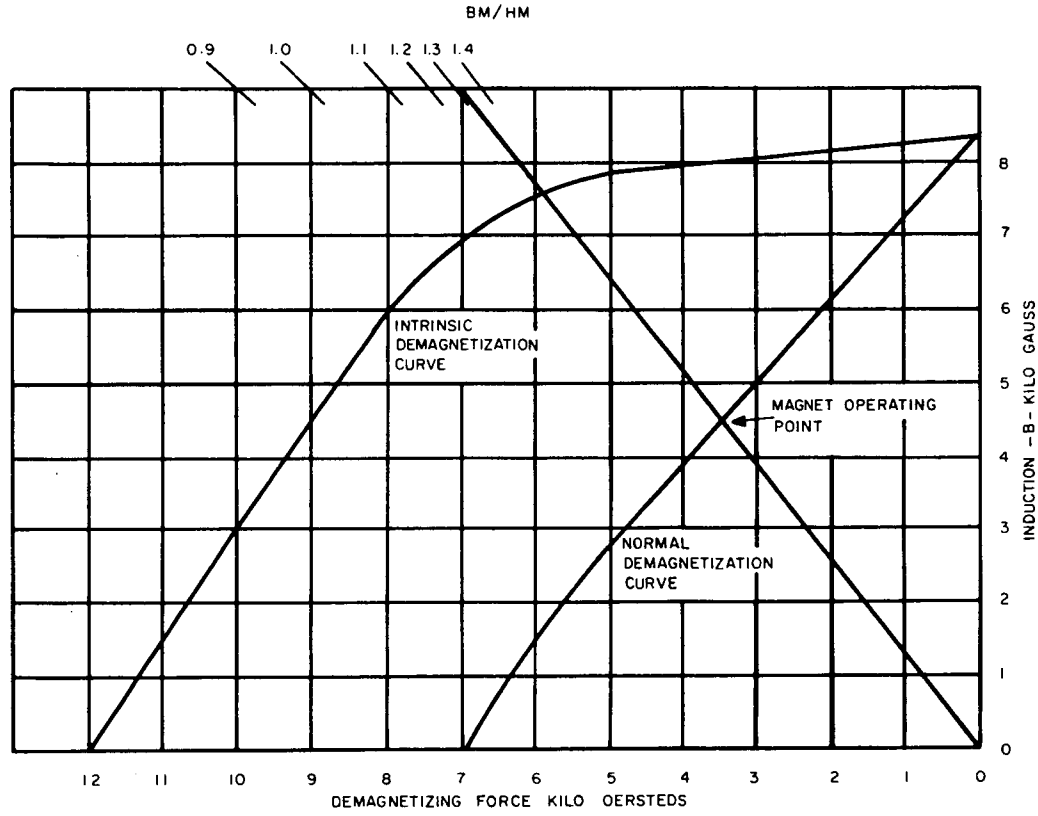

Figure 3-4. Magnet Operating Curve

The flux in the magnet and the airgap flux, previously measured using the sample magnets, were used to determine the leakage factor (ϕ_m/ϕ_g).

$$\frac{\phi_m}{\phi_g} = \frac{11,200}{8,900}$$

$$= 1.26$$

where

ϕ_m = Flux in magnet = $B_m A_m$ = 11,200 lines

ϕ_g = Flux per pole in airgap = 8,900 lines

The number of conductors per phase was obtained using the following equation:

$$K_{T_1} = 22.4 \times 10^{-8} \times Z \times \phi_g \times P/A$$

$$Z = \frac{K_{T_1} \times A}{22.4 \times 10^{-8} \times \phi_g \times P}$$

$$= 1672$$

where

K_{T_1} = Torque constant = 40 oz-in./amp min

Z = Number of conductors per phase

ϕ_g = Flux per pole in airgap = 8,900 lines

P = Number of poles = 12

A = Number of parallel paths = 1

From this calculation, the number of turns per coil (N_1) was determined

$$N_1 = \frac{Z}{(C)\ (2 \text{ conductors/coil})}$$

$$= \frac{1672}{(12)(2)}$$

$$= 69.67$$

where

Z = Number of conductors per phase = 1672

C = Number of coils per phase = 12

To allow some safety factor, use 78 turns per coil (N_2). Calculating the new torque constant (K_{T_2}), then

$$K_{T_2} = K_{T_1} \left(\frac{N_2}{N_1}\right)$$

$$= (40 \text{ oz-in./amp}) \left(\frac{78}{69.67}\right)$$

$$= 44.8 \text{ oz-in./amp}$$

The actual measured torque constant of the motors was 65 ounce-inch/ampere rather than 44.8. The actual torque constant was higher for several reasons:

1. Since the edges of the magnets were not curved to conform to the curvature of the airgap, the average airgap was less than 0.200 inch.

2. Some of the leakage flux still passed through the winding and contributed to the torque.

3. Magnets used in the motors appeared to have more output than the sample magnets.

In order to determine resistance (R), the mean length of the conductor (LMC) was determined as follows:

$$LMC = \frac{(Dia)\,\pi}{P} + \frac{(Dia)\,\pi}{P(3)} + W$$

$$= \frac{3.860\,\pi}{12} + \frac{3.860\pi}{12(3)} + 0.64$$

$$= 2.037 \text{ in.}$$

$$= 0.170 \text{ ft}$$

where

P = number of poles = 12

W = axial width of coil = 0.64 in.

Consider number 29 AWG wire. R/ft for number 29 wire = 0.0812 ohm/ft.

$$R/phase = (LMC)\ Z\ (R/ft)$$

$$= (0.170 \text{ ft})(1872 \text{ conductors})(0.0812 \text{ ohm/ft})$$

$$= 25.8 \text{ ohms}$$

$$R(delta) = 2/3\ (R/phase)$$

$$= 2/3\ (25.8 \text{ ohms})$$

$$= 17.2 \text{ ohms}$$

The actual measured resistance per phase for a motor wound with this winding was 24.4 ohms or 16.3 ohms for the delta.

ARMATURE DESIGN

The armature design consisted of a delta-wound winding and a mechanical support for the winding. The desired generated voltage waveform was shown in Figure 3-1.

Assuming that square wave flux distribution as shown in Figure 3-5 can be obtained from the magnetic design, the armature can be wound with full pitched coils having the conductors evenly distributed over the periphery of the armature shell. Each phase is evenly distributed over 1/3 of a pole span. Therefore, the rotor can move 1/3 of a pole span (60 electrical degrees) with an equal number of conductors in the flux field. This would give a constant generated voltage for 60 electrical degrees. Figure 3-5 shows the air gap flux waveform and the relative position of the armature coils for three rotor positions (through 180°E).

The generated voltage is given by $E = \frac{Z \phi N}{60} \times 10^{-8}$ volts. Assuming a constant speed and the flux distribution shown, the generated voltage in each phase will be proportional to the number of conductors in the magnetic field at that position. The table below was developed to determine the conductors and the polarity of the generated voltage in the conductors for the different rotor positions. The numeral 1 in the table means that all of the conductors for that side of the phase are in the field. A negative number means reversed polarity.

	A	B	C	A^1	B^1	C^1
Position 1	0	1	1	0	1	1
Position 2	1	1	0	1	1	0
Position 3	1	0	-1	1	0	-1

The generated voltage $E = E_b = E_c + E_a$ (Figure 3-5) since one leg of the delta is in parallel with the other two legs.

Position 1 $E_{12} = E_B = 1 + 1 = 2$

$E_{12} = E_c + E_a = 1 + 1 + 0 + 0 = 2$

Position 2 $E_{12} = E_B = 1 + 1 = 2$

$E_{12} = E_c + E_a = 0 + 0 + 1 + 1 = 2$

Position 3 $E_{12} = E_c + E_a = (-)1 + (-)1 + 1 + 1 = 0$

Therefore, the generated voltage across phase B from position 1 to position 2 is constant. The generated voltage decreases linearly from position 2 to position 3. As phase B moves toward the center of the next pole, the generated voltage builds up again but of opposite polarity.

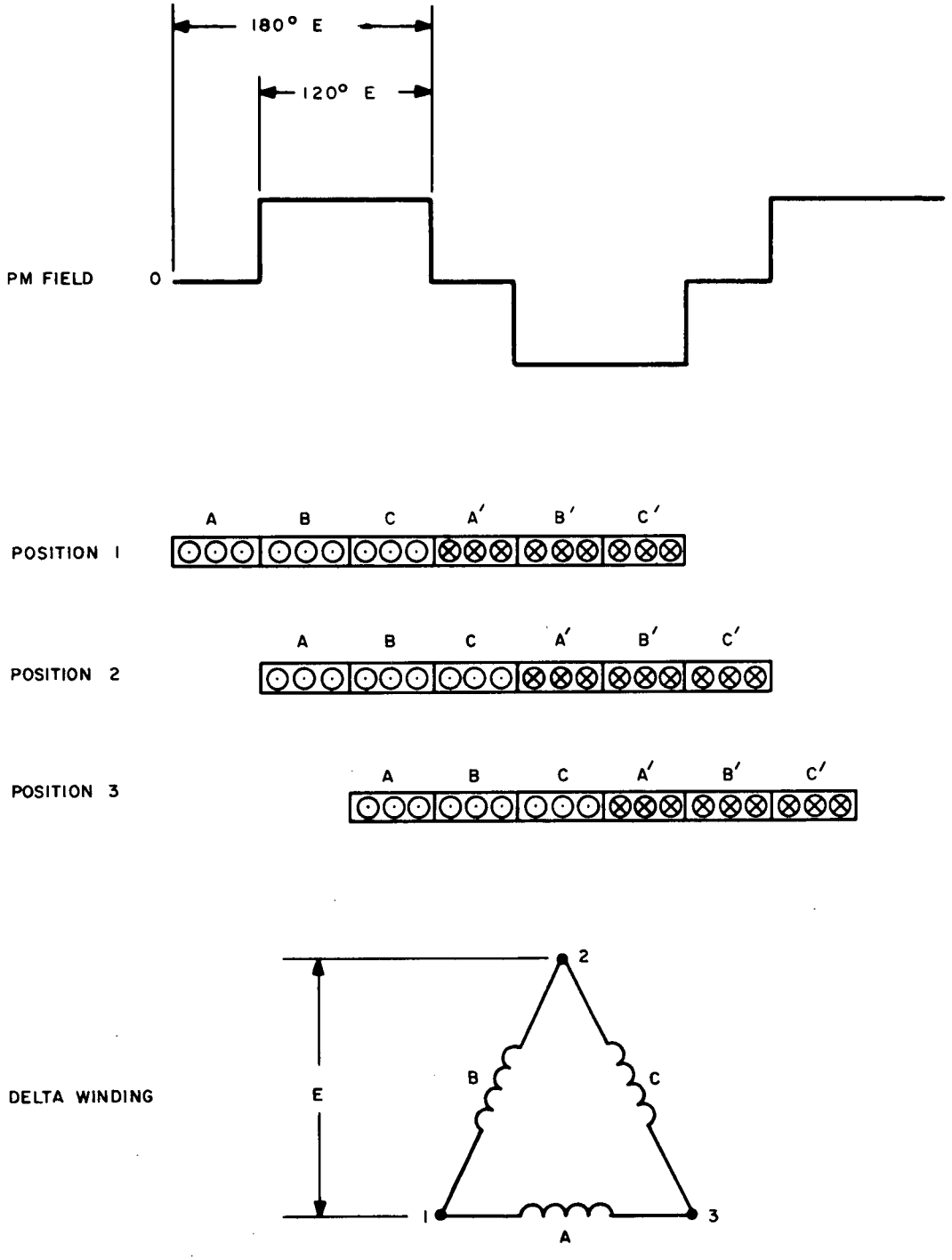

Figure 3-5. Winding and Field Position Diagram

However, the generated voltage waveform obtained was not trapezoidal as desired, but approximately sinusoidal. This waveform will result in higher commutation torque ripple. A sinusoidal rather than trapezoidal waveform was obtained for the following reasons: 1) Due to leakage flux, the flux distribution in the airgap of the motor was trapezoidal close to the magnets but became sinusoidal further away from them (toward the outer ring). Consequently, most of the conductors were cutting a sinusoidal flux rather than the desired square wave flux. 2) The coils for the winding assembly were wound on a rectangular coil form. Because of the tension variation when winding on a rectangular coil form, the coil sides were not straight. As layers of wire built up, the coil sides became more contoured. Consequently, a conductor was not seeing a constant flux across the axial length of the motor, but was integrating the flux over some area based on the curvature of the conductor. This condition could have been improved by extending the coil end turns well past the rotor axial length and by performing additional coil forming after the coils were wound. This would require additional space for end turns and increase the armature resistance.

POSITION SENSORS

F. W. Bell thin film Hall-Pak generators had been tentatively selected for use as angular position sensors. However, after studying the flux distribution waveforms obtained from testing the sample magnets, it appeared that the Hall device waveform was going to be more sinusoidal than trapezoidal. Therefore, consideration was given to using the zero crossover point on the sensor waveform for switching. In order to have as steep a slope as possible to use for switching, a high sensitivity Hall device was desirable. Therefore, the Siemens SV 110-II was choosen. Its characteristics are listed in Table 3-3.

When the first motor was built, it was found that the Hall devices were located close enough to the magnets so that the output waveform was trapezoidal as desired (see Figure 3-1). However, it was decided that larger mechanical gaps were more desirable. Therefore, the Hall devices were moved out of the motor airgap so that the ID of the winding assembly could be increased. The Hall devices were then located 0.045 inch from the side of the magnets and were used to detect the side-leakage flux. The output voltage was approximately sinusoidal and the output varied from Hall device to Hall device, from 45 mv average-to-peak to 150 mv average-to-peak with 10 ma control current.

TABLE 3-3. HALL DEVICE ELECTRICAL SPECIFICATIONS (SIEMENS SV 110-II)

Hall signal probe with vapor-deposited layer

SV 110 is a high sensitivity, high internal resistance Hall device. Within the linear region it may be used as a multiplier, outside it finds application in control and regulating circuits (semiconductor material InSb).

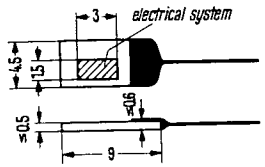

Terminals: Hall voltage: red
Control current: green
Wire length: 100 mm

Weight approx. 0.1 g Dimensions in mm

Maximum ratings

		II	III	
Maximum permissible control current for operation in air	i_{1M}	30	50	mA

Characteristics (T_{amb} = 25 °C)

Rated value of control current for operation in air	i_{1n}	15	2d	mA
Open-circuit Hall voltage at B = 10 kG and i_{1n}	v_{20n}	≧1.0	≧0.8	V
Open-circuit sensitivity referred to $B \rightarrow 0$	K_{0a}	10	5	V/A·kG
Control-side internal resistance	R_{10}	approx.500	approx.200	Ω
Hall-side internal resistance	R_{20}	≦R_{10}	≦R_{10}	Ω
Ohmic zero voltage at i_{1n}	v_{20}	≦10	≦10	mV
Mean temperature coefficient of v_{20} between 0 and 50 °C	β	approx.–1.5	approx.–1.5	%/°C
Temperature coefficient of R_{10} between 0 and 50 °C	α	approx.–1	approx.–1	%/°C
		–40...+80		°C

$v_{20} = f(B)$
R_L/R_{10} = parameter

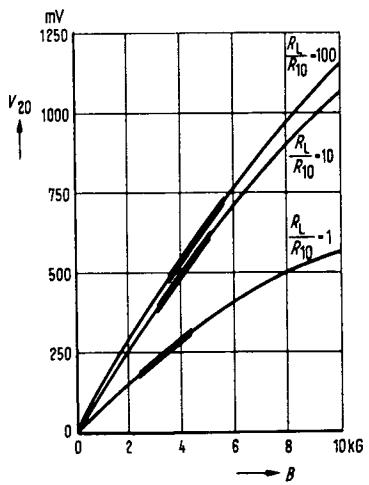

Sensitivity curves
$V_{20}/B = f(i_1)$

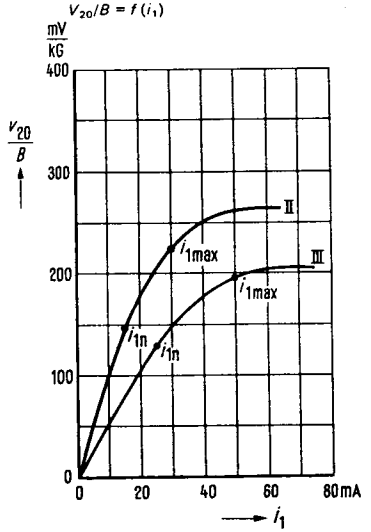

Temperature dependence of Hall voltage
i_1, v_1 = parameter

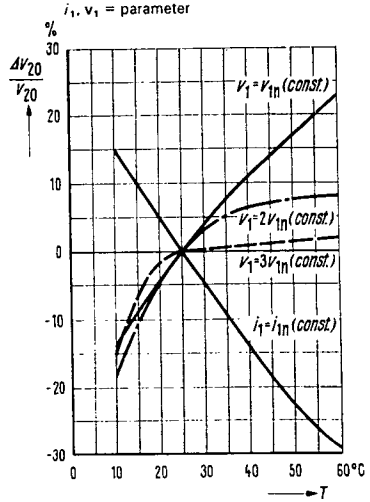

SECTION IV

FABRICATION

The rotor assembly consisted of a magnet assembly, an outer magnetic ring, and aluminum structural elements to connect the two members. The airgap between the outer ring and the magnet assembly was 0.508 centimeters (0.200 inch).

The magnet assembly was made up of twelve (12) samarium cobalt permanent magnets which were cemented onto the OD of an ingot iron ring. Slots were put on the OD of the ring to position the magnets. In an attempt to square up the flux distribution in the airgap, the magnets were left rectangular in shape rather than rounding the edges to conform to the curvature of the airgap.

The samarium cobalt magnets were purchased already magnetized. Necessary care was taken in handling and assembling these magnets due to the high magnetic pull and brittle nature of the magnets.

After the magnet assembly was placed on the aluminum support, the outer ring was cemented into place. A nonmagnetic shim had to be placed in the airgap during assembly to prevent the outer ring from being pulled into the magnets.

The winding assembly was constructed by cementing individual coils onto an epoxy-glass ring, connecting the coils, and potting the assembly. An aluminum mounting ring with terminals was provided on one end. After the winding assembly was potted, the ID of the assembly was machined.

The coils were wound onto a rectangular coil form. The wire was coated with a cement as it was wound so that the coil would retain its shape when removed from the coil form.

An engineering model was fabricated with the Hall devices in the airgap of the motor. Slots were placed in the epoxy-glass ring to locate the Hall devices. Hall devices were assembled after the potting and final machining of the winding assembly. This design provided for the minimum radial clearance of 0.006 inch.

The configuration was revised to provide larger mechanical clearances. Hall devices were mounted into an epoxy ring so that the OD of the ring would

pilot into the ID of the winding assembly mounting ring. The sensor ring assembly was mounted against the test fixture with three screws. The test fixture was slotted so that the position of the sensor assembly would be adjustable for phasing the sensors with the winding for best commutation.

Hall devices were located nominally 0.045 inch axially from the magnet assembly and thus sensed the side leakage flux. The OD of the winding assembly was reduced from 4.045 inches to 4.025 inches by changing the wire size of the winding from 29 gage to 30 gage. With the Hall devices removed from the ID of the winding assembly, the ID was increased to 3.790 inches.

These changes required making both a new mold for the winding assembly and a mold for the sensor ring as well as modifying the test fixture.

The winding assembly was potted with Scotchcast Resin 251, which is a filled epoxy. It is a medium viscosity, rigid, class F (155°C) resin system. The resin was warmed in order to lower its viscosity for maximum impregnating ability. Nevertheless, voids still occurred and had to be filled.

The sensor ring was made of the same epoxy so as to be compatible. Each Hall device was cemented into a slot in the sensor ring and then covered with a conformal coating for protection. (The Hall devices were found to be extremely fragile.)

SECTION V

TESTING

INTRODUCTION

Tests were performed to evaluate each unit manufactured and to evaluate flux distribution with various configurations. The results of the tests are presented in this section.

FIRST UNIT - ENGINEERING MODEL (EM)

During final machining a wire was nicked causing one phase to be open. Test data on the unit was obtained from the two good phases and is presented in Figures 5-1 through 5-4. Mechanical data is listed below.

Motor Characteristics (Hall Devices in Airgap):

No. of Turns	78 turns per coil
Gage Wire	29
Resistance (Delta)	16.3 ohms
Voltage Constant	0.47 volts/radian/second peak

Breakdown of Weight:

Rotor Assembly

Outer Ring	105.7 gm
Magnets	146.4 gm
Yoke	67.2 gm
Housing	177.0 gm
Clamp Ring	12.0 gm
Total Rotor Assembly	508.3 gm

Winding Assembly

Terminal Ring	27.9 gm
Wire	165.0 gm
Epoxy	14.1 gm
Total Winding Assembly	216.0 gm

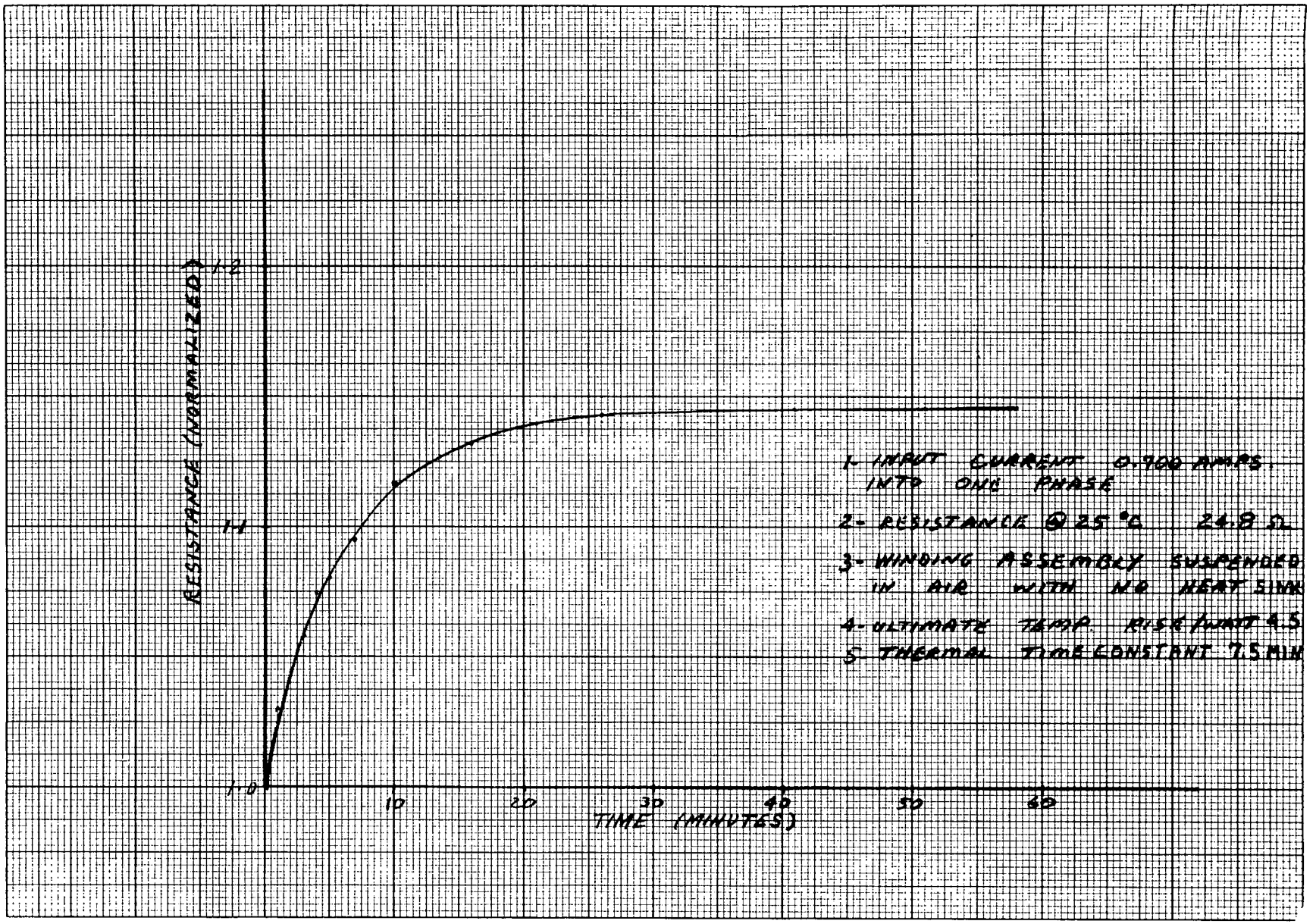

Figure 5-1. Ironless Armature Winding Assembly
(Resistance vs Time)

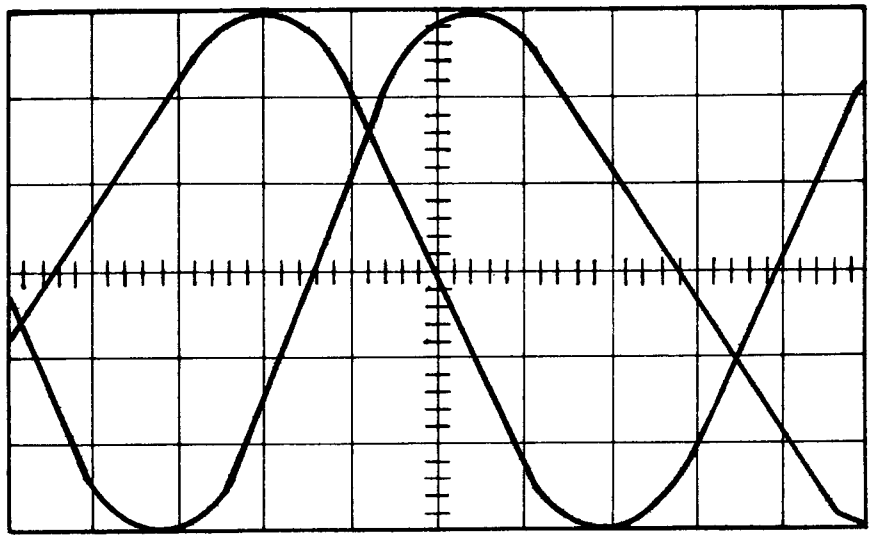

Figure 5-2. EM Generated Voltage Waveform,
Speed = 12.45 radians/second.
Voltage Constant = 0.474 volts/radian/second peak.

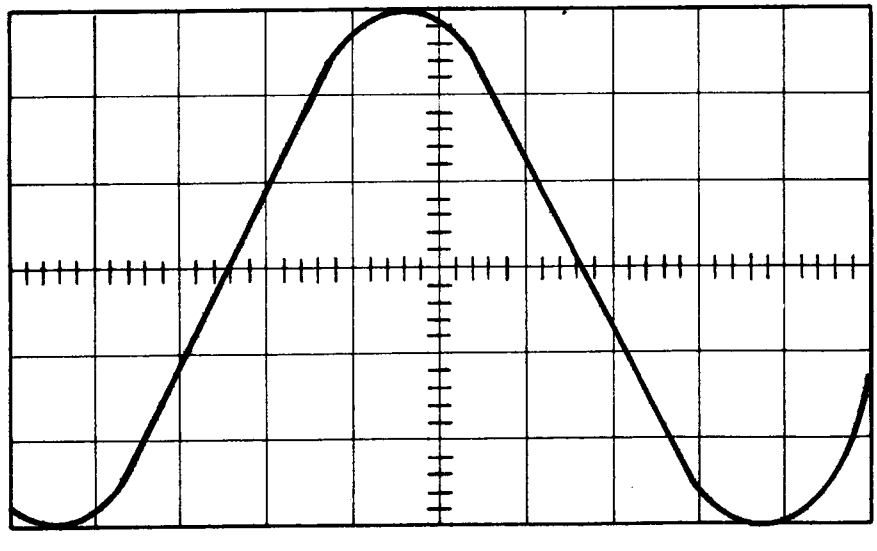

Figure 5-3. EM Generated Voltage Waveform of Two Phases Added, Voltage Constant = 0.50 volts/radian/second peak.

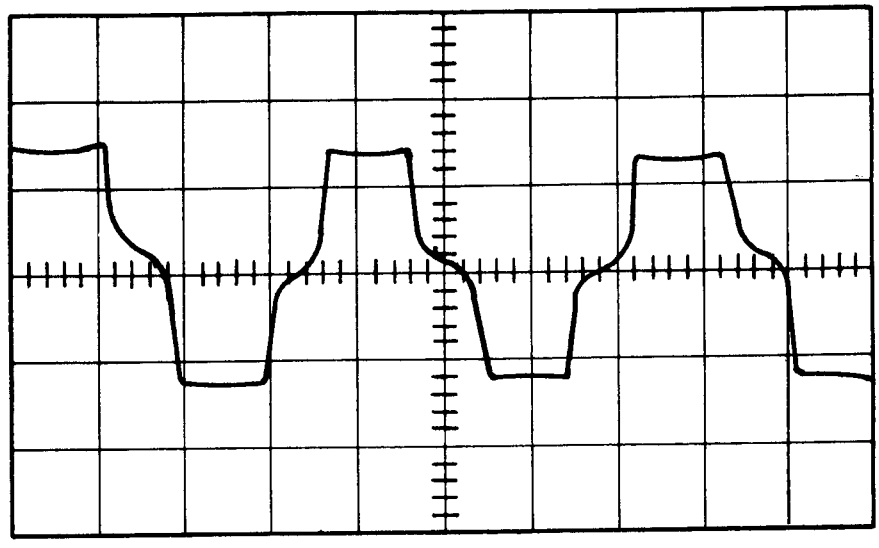

Figure 5-4. EM Hall Device Waveform,
Peak-to-Peak Voltage = 1.35 volts.

Motor

Rotor Assembly	508.3 gm
Winding Assembly	216.0 gm
Total Motor	724.3 gm or 1.6 lb

Wire and Magnetic Parts

Outer Ring	105.7 gm
Magnets	146.4 gm
Yoke	67.2 gm
Wire	165.0 gm
Total Wire & Magnetic Parts	484.3 gm or 1.07 lb

The winding temperature rise was measured by suspending the winding assembly in the air and measuring the voltage and current at time intervals (see Figure 5-1). A current of 0.700 ampere was applied to one phase. The ultimate temperature rise per watt was 4.5 watts per degree centigrade. The thermal time constant was 7.5 minutes.

SERIAL NUMBER 1 (SN 1)

Test data for serial number 1 is presented in Figures 5-5 through 5-7. Mechanical data is listed below:

Serial Number 1 - Ironless Armature Torquer

Motor Characteristics

No. of Turns	78 turns per coil
Gage Wire	30
Resistance (Delta)	20.7 ohms
Voltage Constant	0.50 volts/radian/second peak
Torque Constant (Peak)	70.7 ounce-inches/ampere

Breakdown of Weight

Armature (Total After Final Machining)	177.3 gm
Coils	111.1 gm
Mounting Ring	28.3 gm
Epoxy plus Phonolic Ring for Coil Support	37.9 gm
Rotor Assembly (Less Alum. Housing)	324.6 gm
Magnets	152.1 gm
Yoke	67.1 gm
Outer Ring	105.4 gm
Aluminum Housing	178.1 gm
Sensor Assembly	35.8 gm
Total Weight Less Aluminum Housing	537.7 gm
Total Weight Including Aluminum Housing	715.8 gm
Total Weight of Electrical and Magnetic Parts (Wire, Iron, Magnets)	435.7 gm

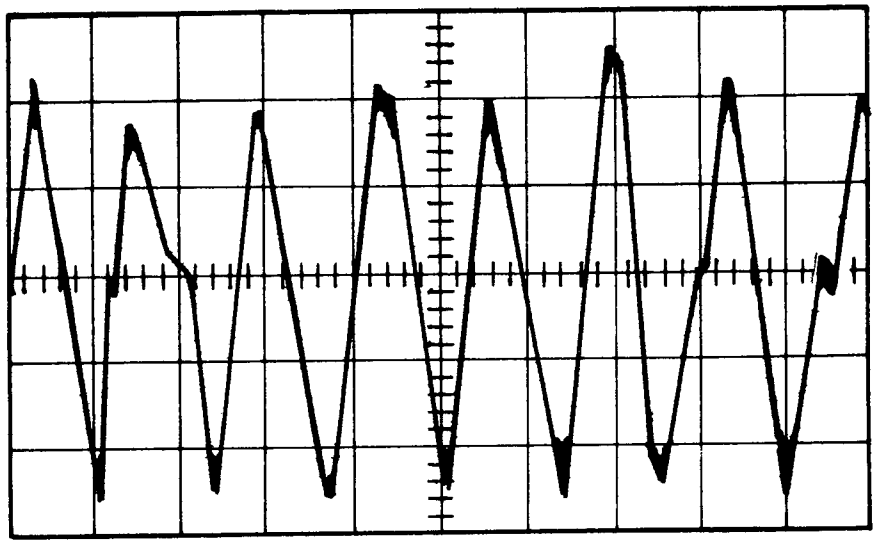

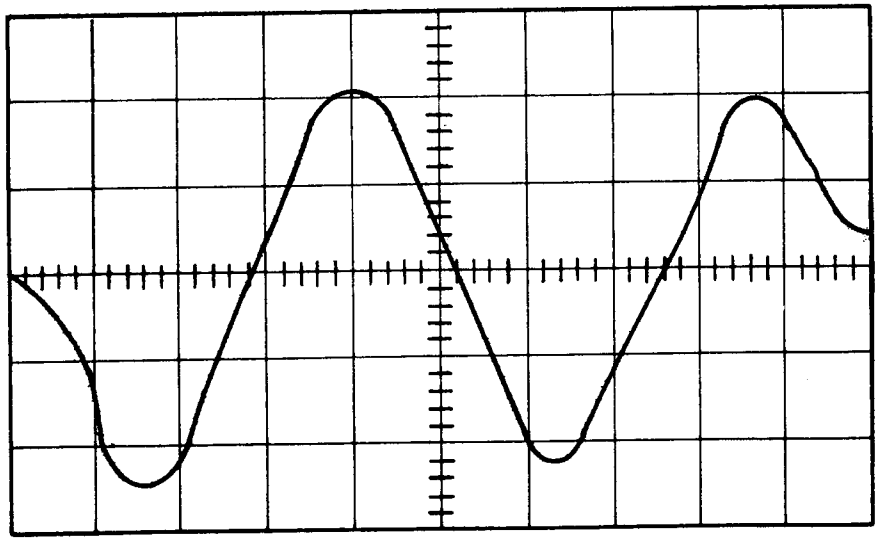

Figure 5-5. SN 1 Hall Device Waveforms,
Input Current: 10 ma
Scale: 50 mv/cm

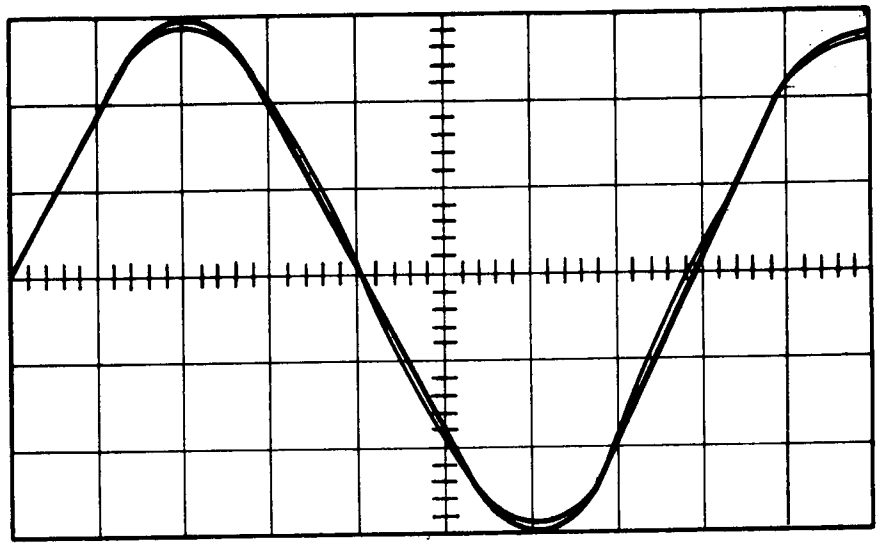

Figure 5-6. SN 1 Generated Voltage Waveform, Phase 1 and Phase 2 and Phase 3
Scale: 5 v/cm and 5 ms/cm

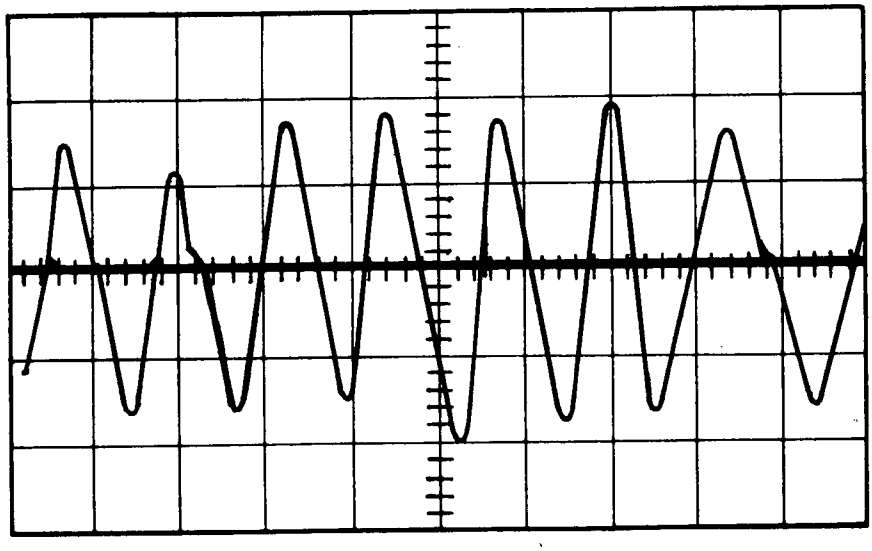

Figure 5-7. SN 1 Hall Device Output,
Scale: 50 mv/cm and 50 ms/cm

SERIAL NUMBERS 2 THROUGH 4

Serial numbers 2 through 4 were manufactured just as serial number 1. Serial number 2 had a nicked wire which appeared to be just insulation scraped off and which did not effect performance. A drawing change was necessary to insure that this did not happen again.

The test data for serial number 2 (SN 2) is presented in Table 5-1 and Figures 5-8 through 5-10; test data for serial number 3 (SN 3) is presented in Table 5-2 and Figures 5-11 through 5-13, and test data for serial number 4 (SN 4) is presented in Table 5-3 and Figures 5-14 through 5-16.

TABLE 5-1. TEST DATA IRONLESS ARMATURE TORQUE
MOTOR GSF SPECIFICATION NO. S-721-P-4
SPERRY PART NO. 700-00245 SN 2

1. Insulation Resistance @ 100 VDC

   ϕ_1 to Case >1500 Megohms

   ϕ_2 to Case >1500 Megohms

   ϕ_3 to Case >1500 Megohms

2. Resistance @ 25°C

   ϕ_1 31.4 Ohms

   ϕ_2 31.5 Ohms

   ϕ_3 31.5 Ohms

3. Inductance (Disassemblied - Winding Only)

   ϕ_1 3.04 Millihenrys

   ϕ_2 3.04 Millihenrys

   ϕ_3 3.04 Millihenrys

4. Inductance (Assemblied)

   ϕ_1 4.60 Millihenrys

   ϕ_2 4.61 Millihenrys

   ϕ_3 4.61 Millihenrys

   Delta 4.14 Millihenrys

TABLE 5-1 (Cont)

5. Peak Back EMF Constant

ϕ_1 0.5 Volts/Rad/Sec

ϕ_2 0.5 Volts/Rad/Sec

ϕ_3 0.5 Volts/Rad/Sec

Delta 0.5 Volts/Rad/Sec

6. Peak Output from Hall Device (10 ma input green leads)

	HD1	HD2	HD3
Maximum	108 mv	60 mv	148 mv
Minimum	80 mv	47 mv	117 mv

7. Weight

Stator Assembly (PN 700-00212) 173 grams

Rotor Assembly (PN 700-00191) 504 grams

Hall Device Assembly (PN 700-00244) 43 grams

Tester T. Watson

Date 5/30/72

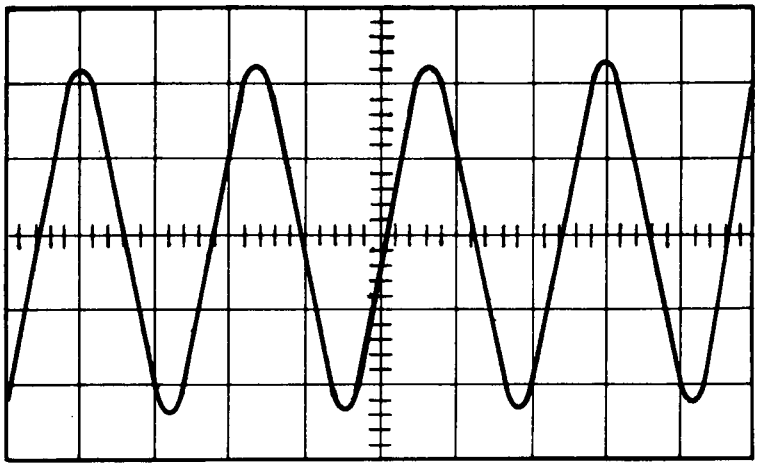

Figure 5-8. SN 2 Generated Voltage Waveform Across Delta,
Scale: 5 v/cm and 20 ms/cm

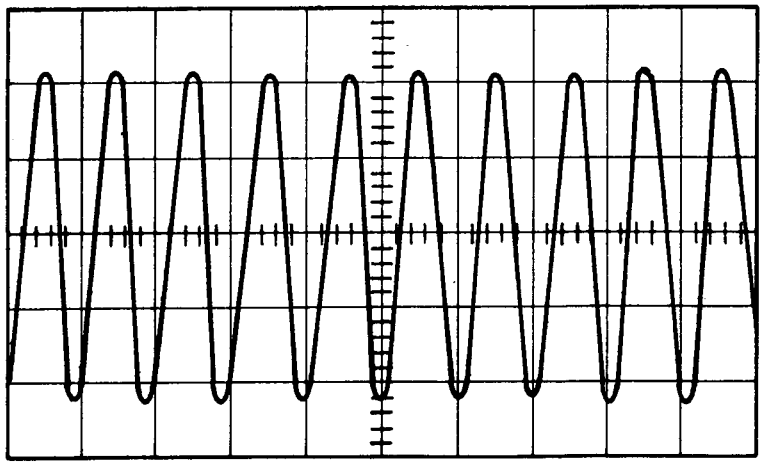

Figure 5-9. SN 2 Generated Voltage Waveform for Ø1,
Scale: 5 v/cm and 50 ms/cm

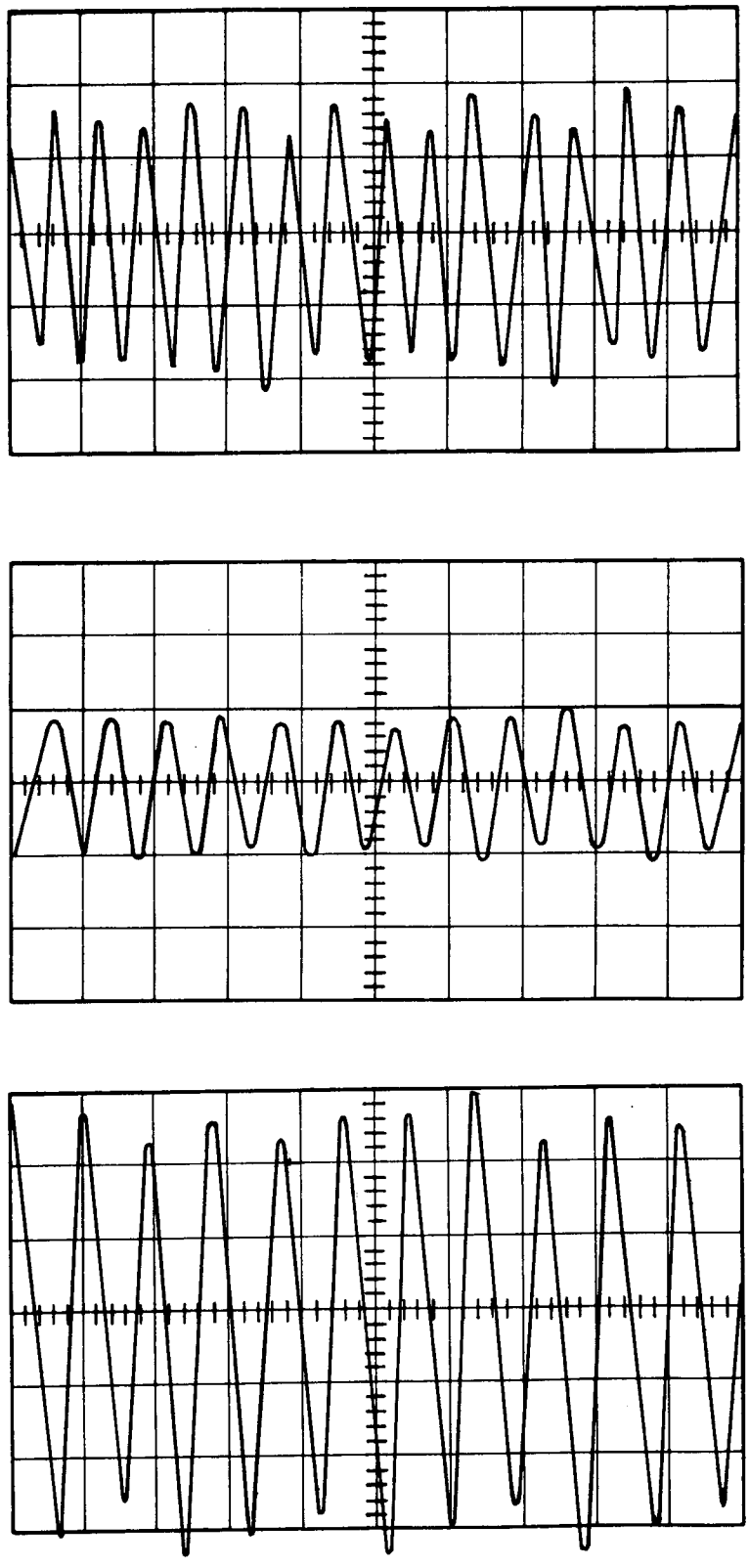

Figure 5-10. SN 2 Hall Device Waveforms,
Input Current: 10 ma - Scale: 50 mv/cm

TABLE 5-2. TEST DATA IRONLESS ARMATURE TORQUE
MOTOR GSF SPECIFICATION NO. S-721-P-4
SPERRY PART NO. 700-00245 SN 3

1. Insulation Resistance @ 100 VDC

   ϕ_1 to Case $\geq 100,000$ Megohms

   ϕ_2 to Case $\geq 100,000$ Megohms

   ϕ_3 to Case $\geq 100,000$ Megohms

2. Resistance @ 25°C

   ϕ_1 30.80 Ohms

   ϕ_2 30.85 Ohms

   ϕ_3 30.40 Ohms

3. Inductance (Disassemblied - Winding Only)

   ϕ_1 3.051 Millihenrys

   ϕ_2 3.053 Millihenrys

   ϕ_3 3.039 Millihenrys

4. Inductance (Assemblied)

   ϕ_1 4.464 Millihenrys

   ϕ_2 4.500 Millihenrys

   ϕ_3 4.330 Millihenrys

   Delta 3.398 Millihenrys

5. Peak Back EMF Constant

   ϕ_1 0.5 Volts/Rad/Sec

   ϕ_2 0.5 Volts/Rad/Sec

   ϕ_3 0.5 Volts/Rad/Sec

   Delta 0.5 Volts/Rad/Sec

Leads to winding terminals reversed. Correct phasing for delta is as follows:

A	3-6
B	2-4
C	1-5

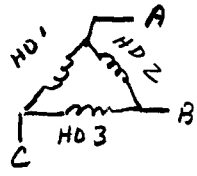

NOTE: The rotor assembly for this motor contains the outer ring that had the overhang reduced to .015 inches.

TABLE 5-2 (Cont)

6. Peak Output from Hall Device (10 ma input green leads)

	HD1	HD2	HD3
Maximum	135mV	89mV	110 mV
Minimum	100mV	68mV	95mV

7. Weight

Stator Assembly (PN 700-00212) _____ grams

Rotor Assembly (PN 700-00191) _____ grams

Hall Device Assembly (PN 700-00244) _____ grams

Tester J J Walter

Date 6/23/72

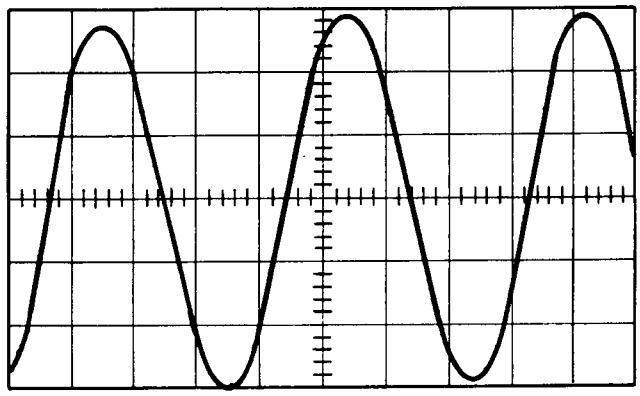

Figure 5-11. SN 3 Generated Voltage Waveform Across Delta, Scale: 5 v/cm and 10 ms/cm

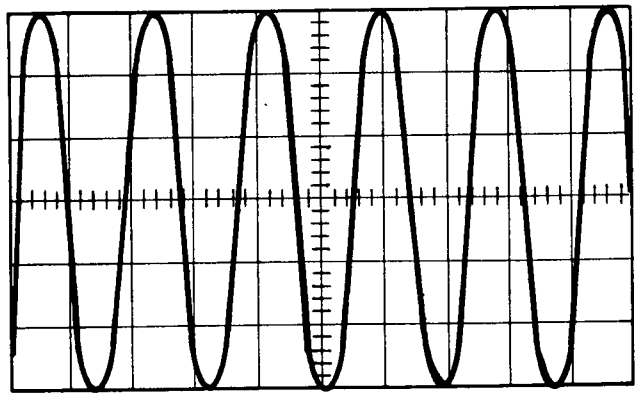

Figure 5-12. SN 3 Generated Voltage Waveform for Ø1, Scale: 5 v/cm and 20 ms/cm

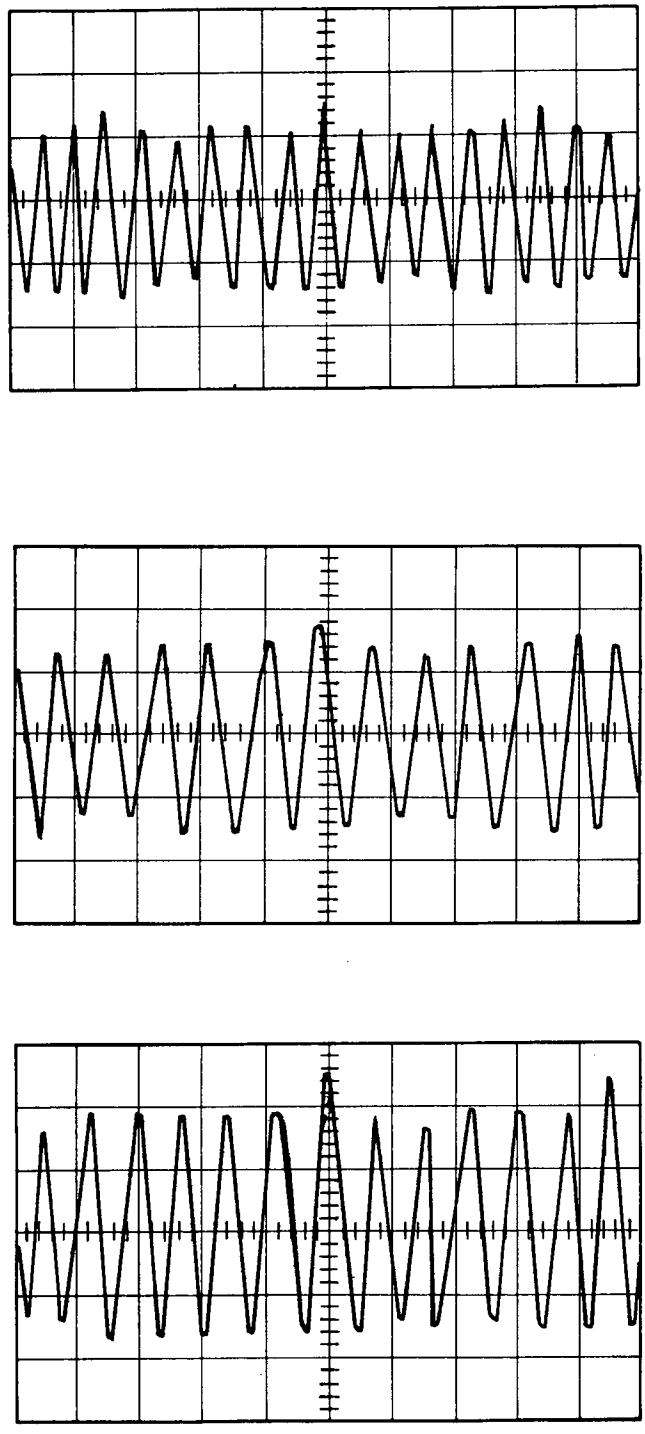

Figure 5-13. SN 3 Hall Device Waveforms, Input Current: 10 ma - Scale: 50 mv/cm

TABLE 5-3. TEST DATA IRONLESS ARMATURE TORQUE
MOTOR GSF SPECIFICATION NO. S-721-P-4
SPERRY PART NO. 700-00245 SN 4

1. Insulation Resistance @ 100 VDC

   ϕ_1 to Case $>200,000$ Megohms

   ϕ_2 to Case $>200,000$ Megohms

   ϕ_3 to Case $>200,000$ Megohms

2. Resistance @ 25°C

   ϕ_1 31.5 Ohms

   ϕ_2 31.4 Ohms

   ϕ_3 31.3 Ohms

3. Inductance (Disassemblied - Winding Only)

   ϕ_1 3.024 Millihenrys

   ϕ_2 3.018 Millihenrys

   ϕ_3 3.02 Millihenrys

4. Inductance (Assemblied)

   ϕ_1 4.45 Millihenrys

   ϕ_2 4.46 Millihenrys

   ϕ_3 4.49 Millihenrys

   Delta 4.15 Millihenrys

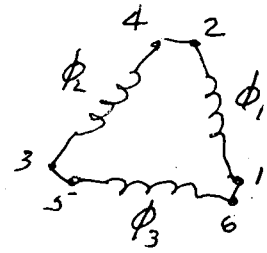

5. Peak Back EMF Constant

   ϕ_1 .43 Volts/Rad/Sec

   ϕ_2 .46 Volts/Rad/Sec

   ϕ_3 .46 Volts/Rad/Sec

   Delta .47 Volts/Rad/Sec

		Low		High
HD 1	ϕ_3	(3-5	-	1-6)
HD 2	ϕ_2	(4-2	-	3-5)
HD 3	ϕ_3	(1-6	-	4-2)

TABLE 5-3 (Cont)

6. Peak Output from Hall Device (10 ma input green leads)

	HD1	HD2	HD3
Maximum	68 MV	115 MV	88 MV
Minimum	45 MV	88 MV	50 MV

7. Weight

Stator Assembly (PN 700-00212) 181.7 grams

Rotor Assembly (PN 700-00191) 502 grams

Hall Device Assembly (PN 700-00244) 43 grams

Tester J. J. Watson

Date 7/14/72

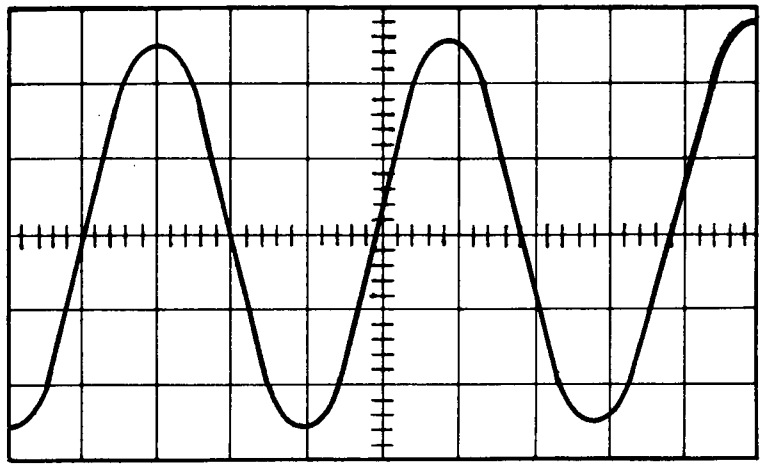

Figure 5-14. SN 4 Generated Voltage Waveform Across Delta, Scale: 5 v/cm and 10 ms/cm

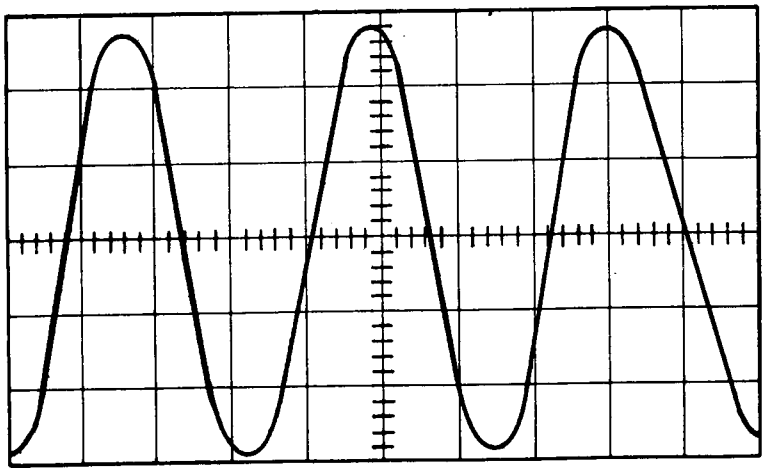

Figure 5-15. SN 4 Generated Voltage Waveform for Ø3, Scale: 5 v/cm and 10 ms/cm

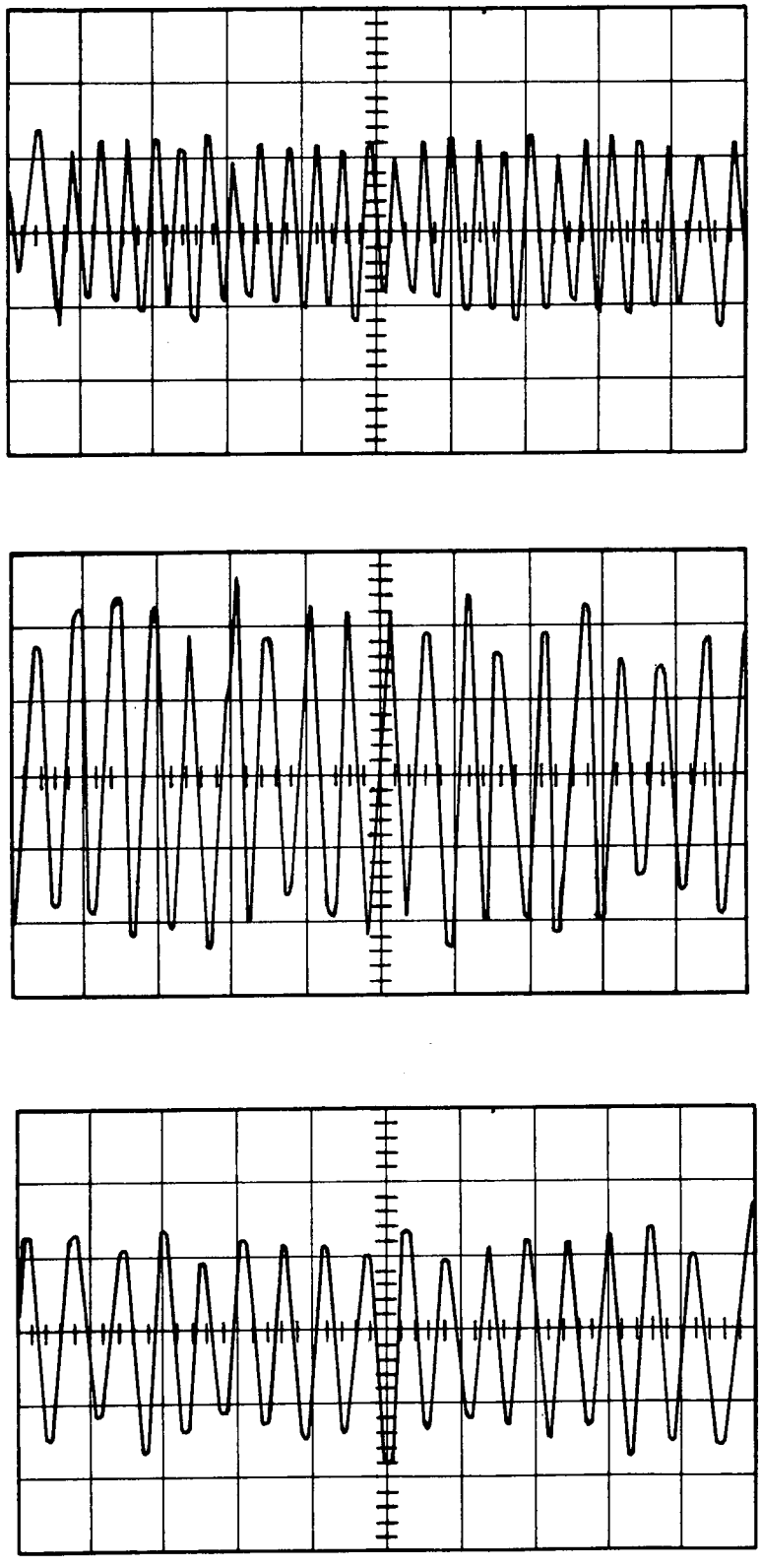

Figure 5-16. SN 4 Hall Device Waveforms,
Input Current: 10 ma - Scale: 50 mv/cm

FLUX DISTRIBUTION EVALUATION

The sample magnets were mounted into various configurations to study the flux distribution. The data obtained is presented in Figures 5-17 through 5-26.

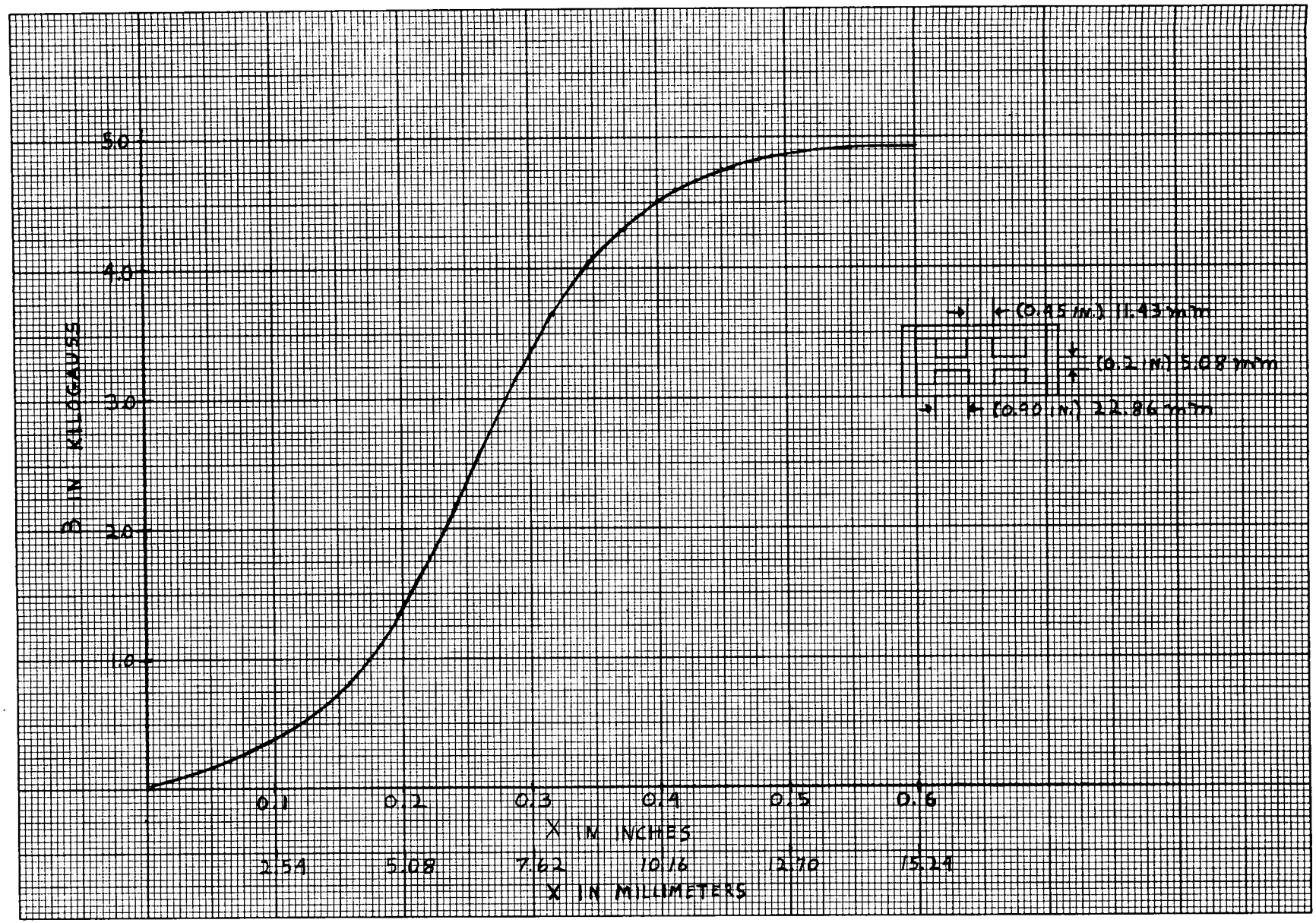

Figure 5-17. Flux Distribution Curve For Magnet Width of 22.86 mm (0.9 in.)

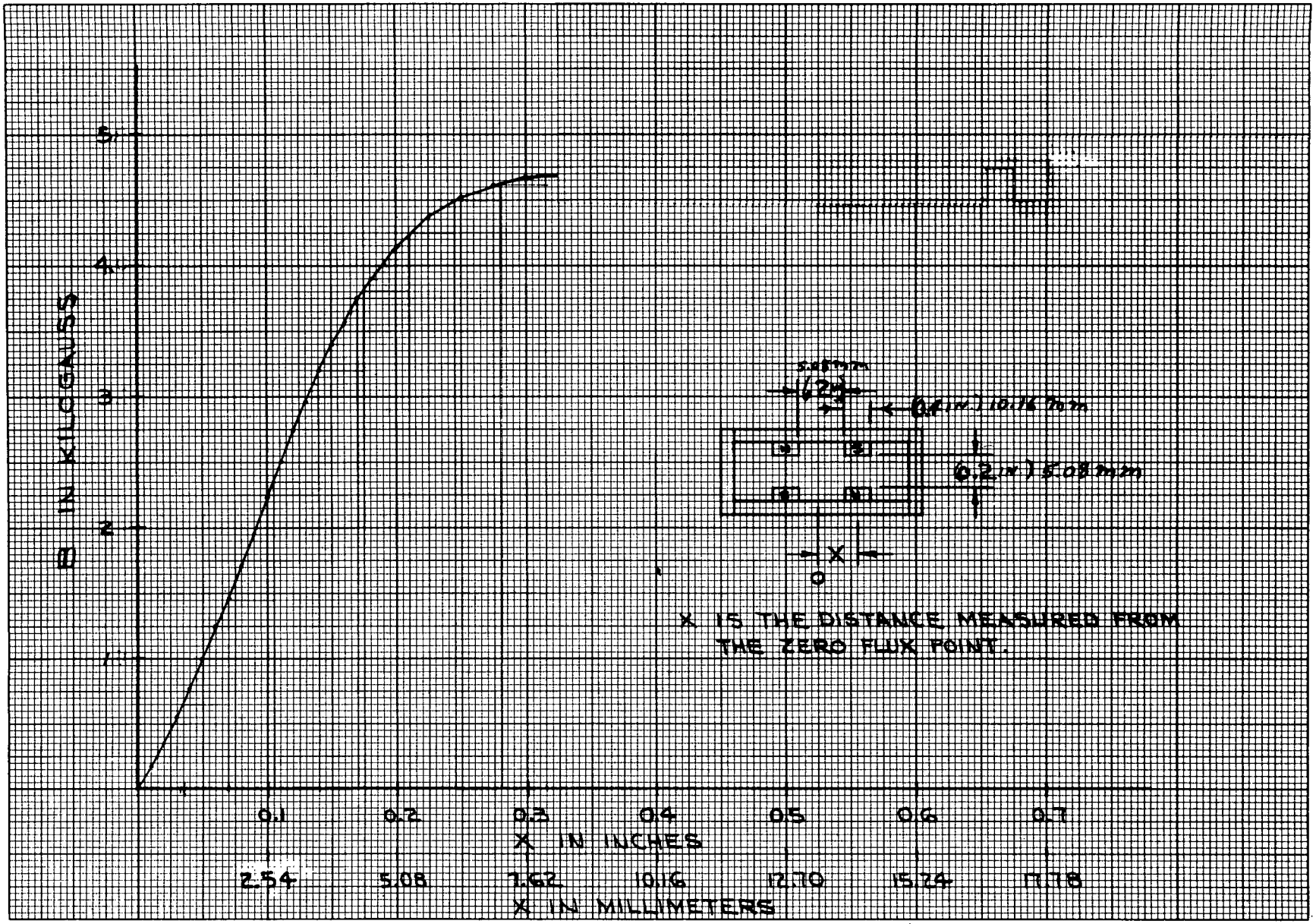

Figure 5-18. Flux Distribution Curve For Magnet Width of 10.16 mm (0.4 in.)

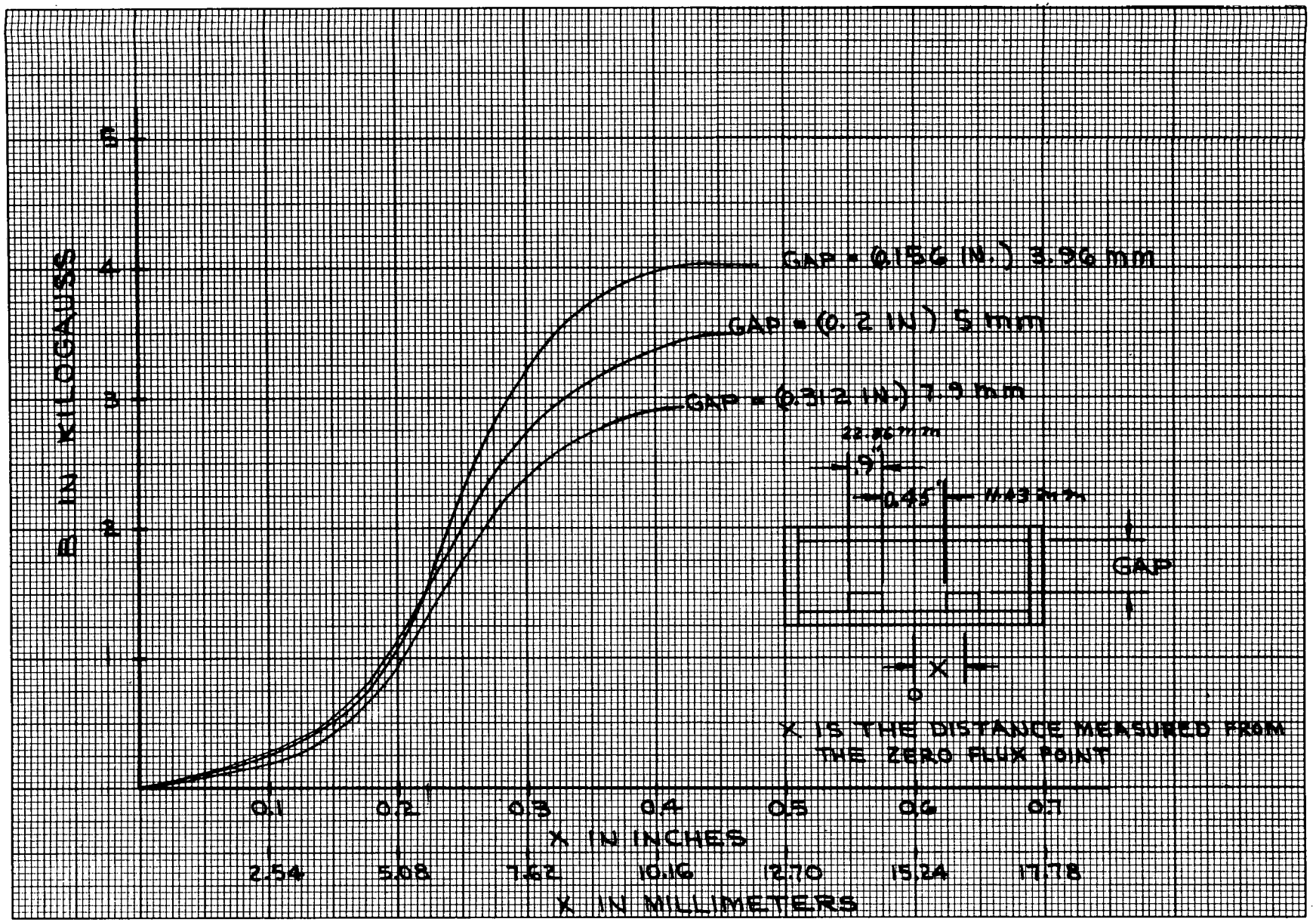

Figure 5-19. Flux Distribution as Magnet Spacing is Varied For Single Magnet Configuration

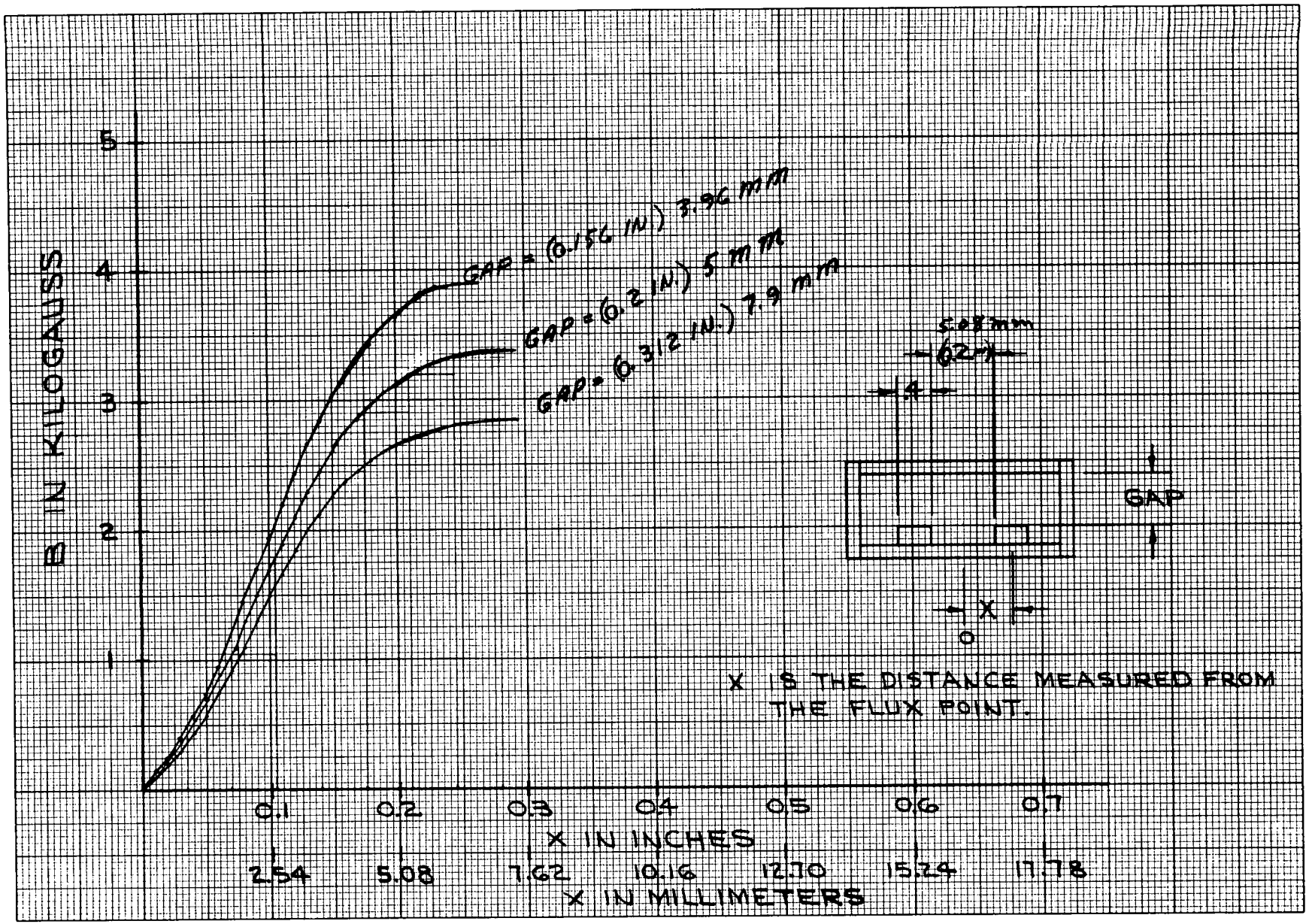

Figure 5-20. Flux Distribution as Airgap is Varied For Single Magnet Configuration

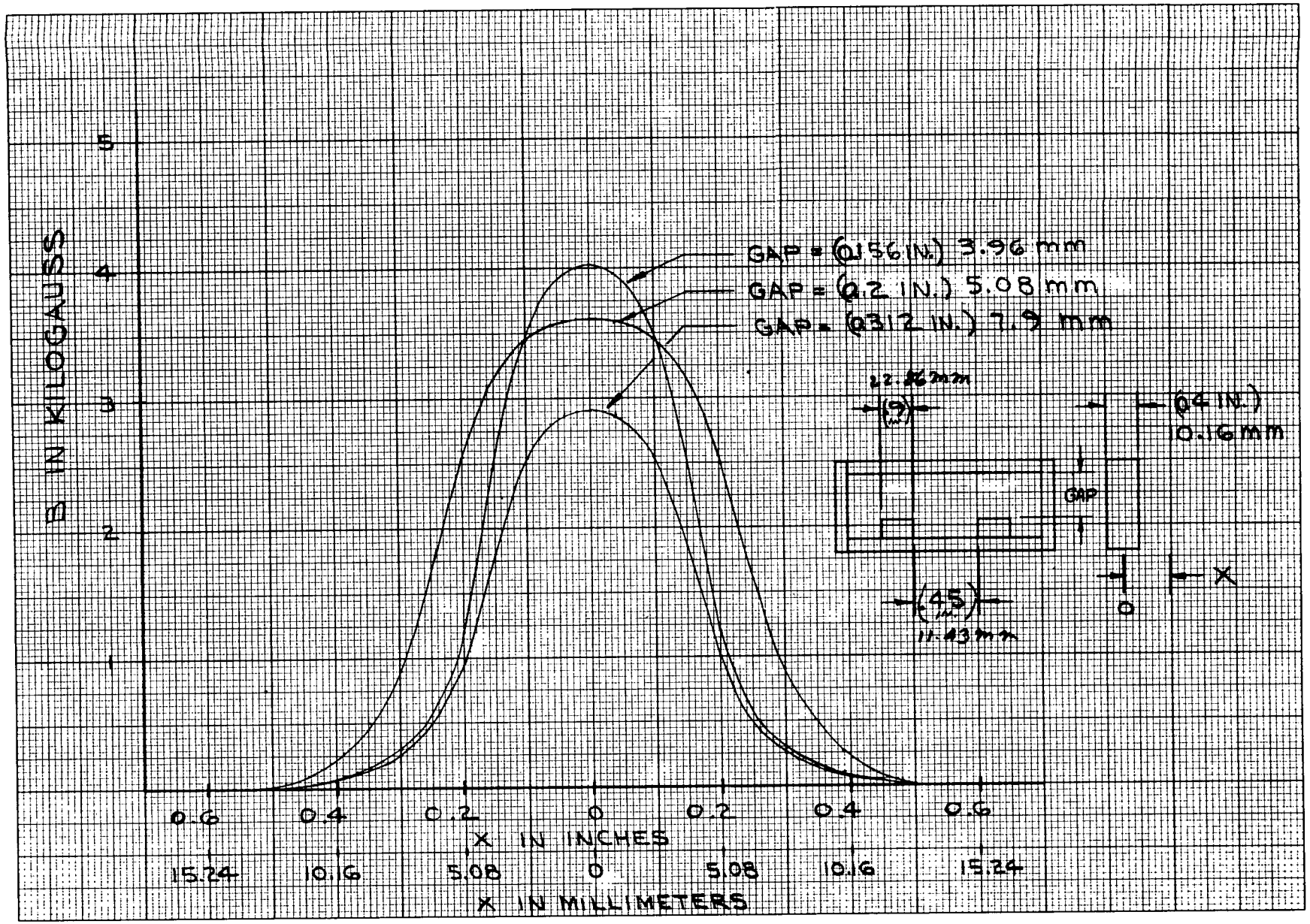

Figure 5-21. Flux Distribution in Axial Direction
For Single Magnet Configuration

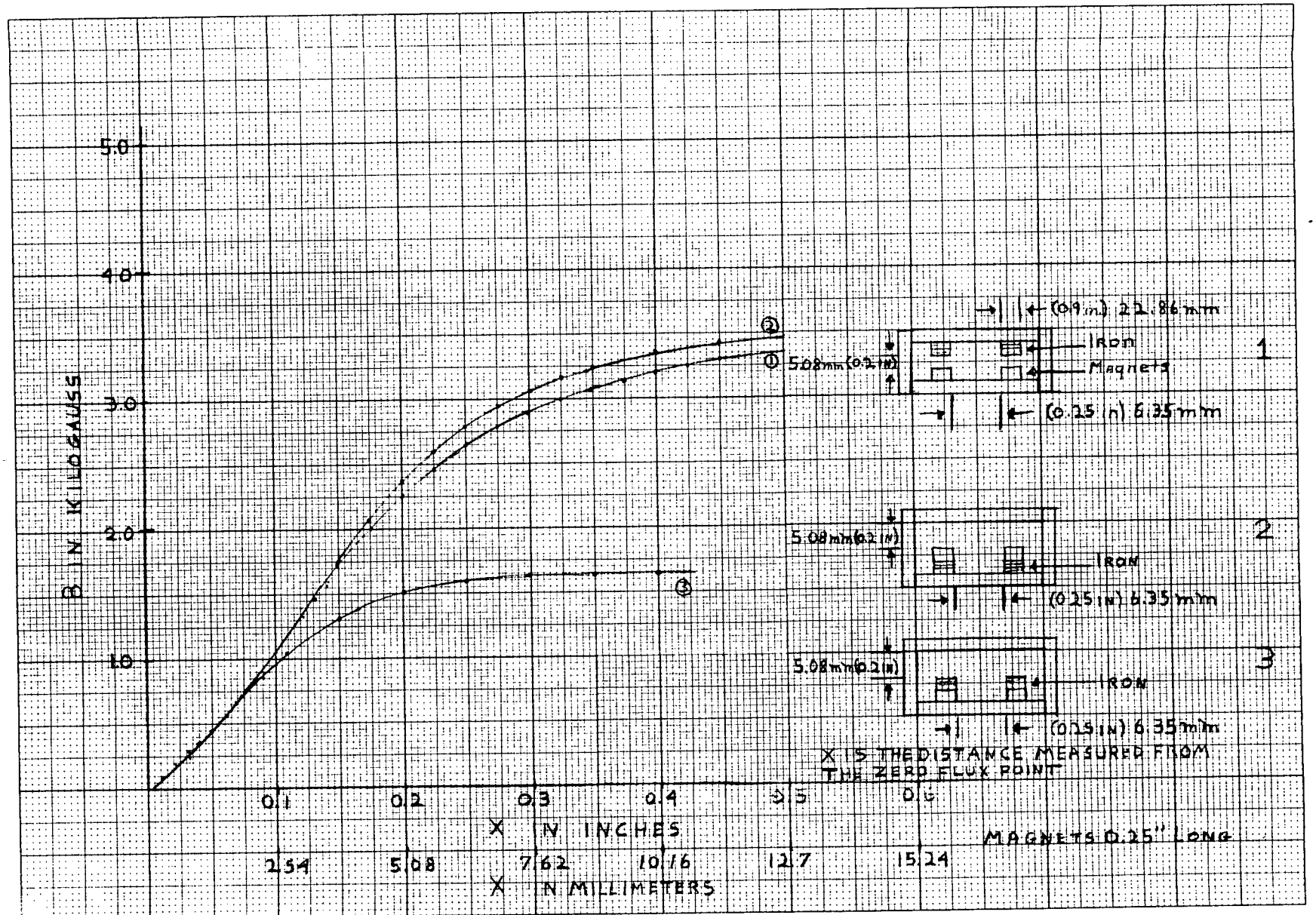

Figure 5-22. Flux Distribution Curve Using Two Magnets and Two Iron Pole Pieces

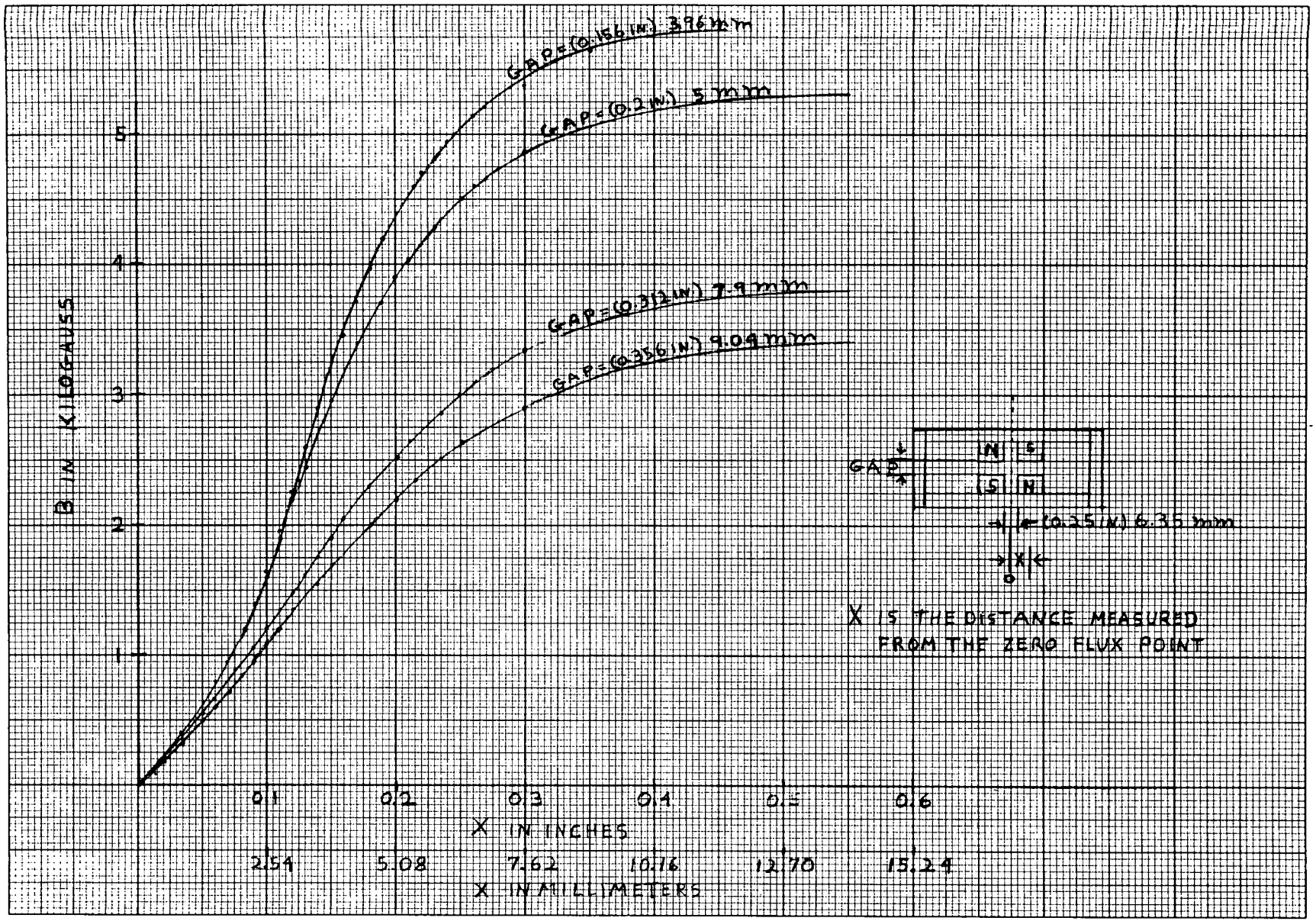

Figure 5-23. Flux Distribution as Airgap is Varied For Double Magnet Configuration

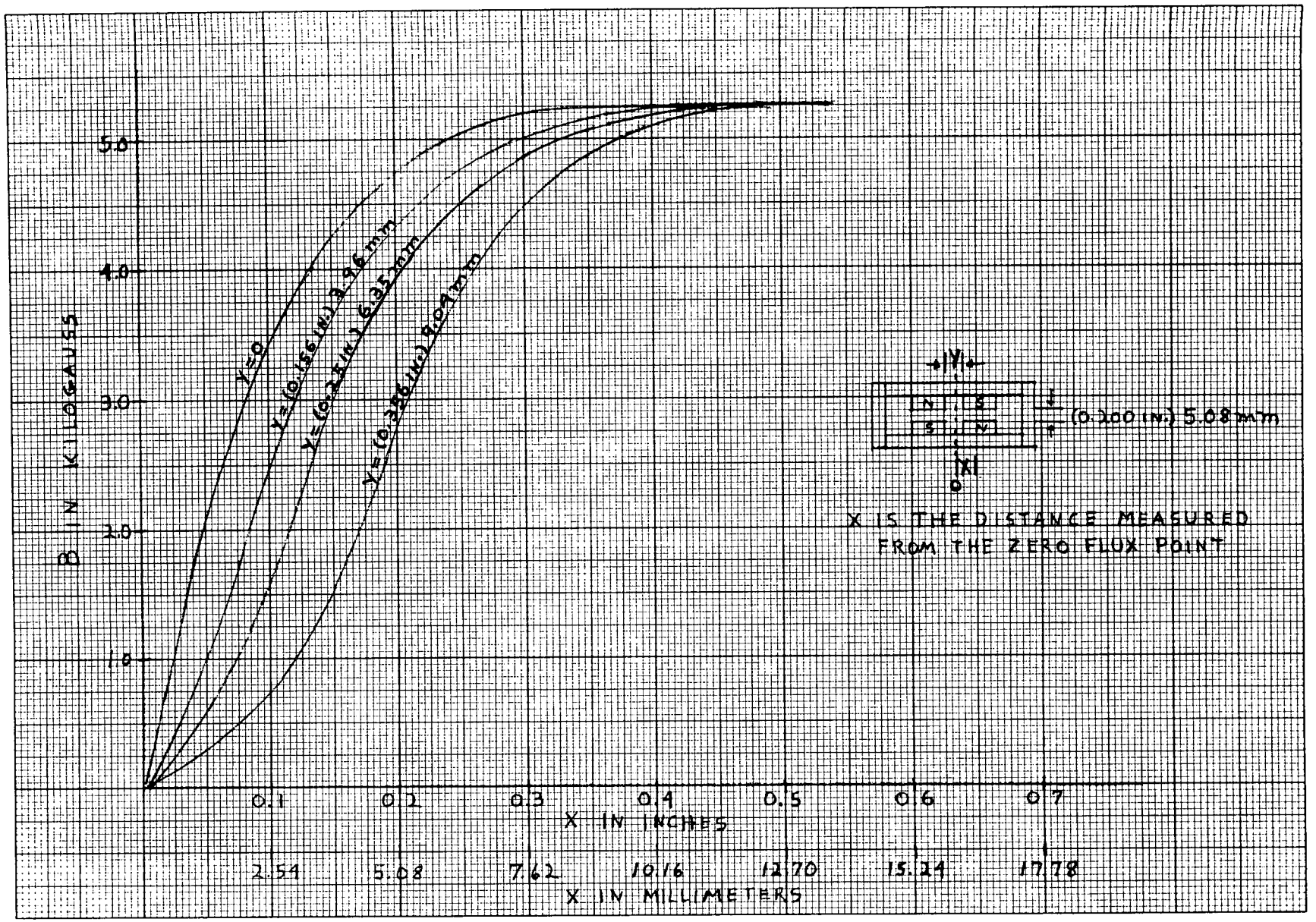

Figure 5-24. Flux Distribution as Magnet Spacing is Varied For Double Magnet Configuration

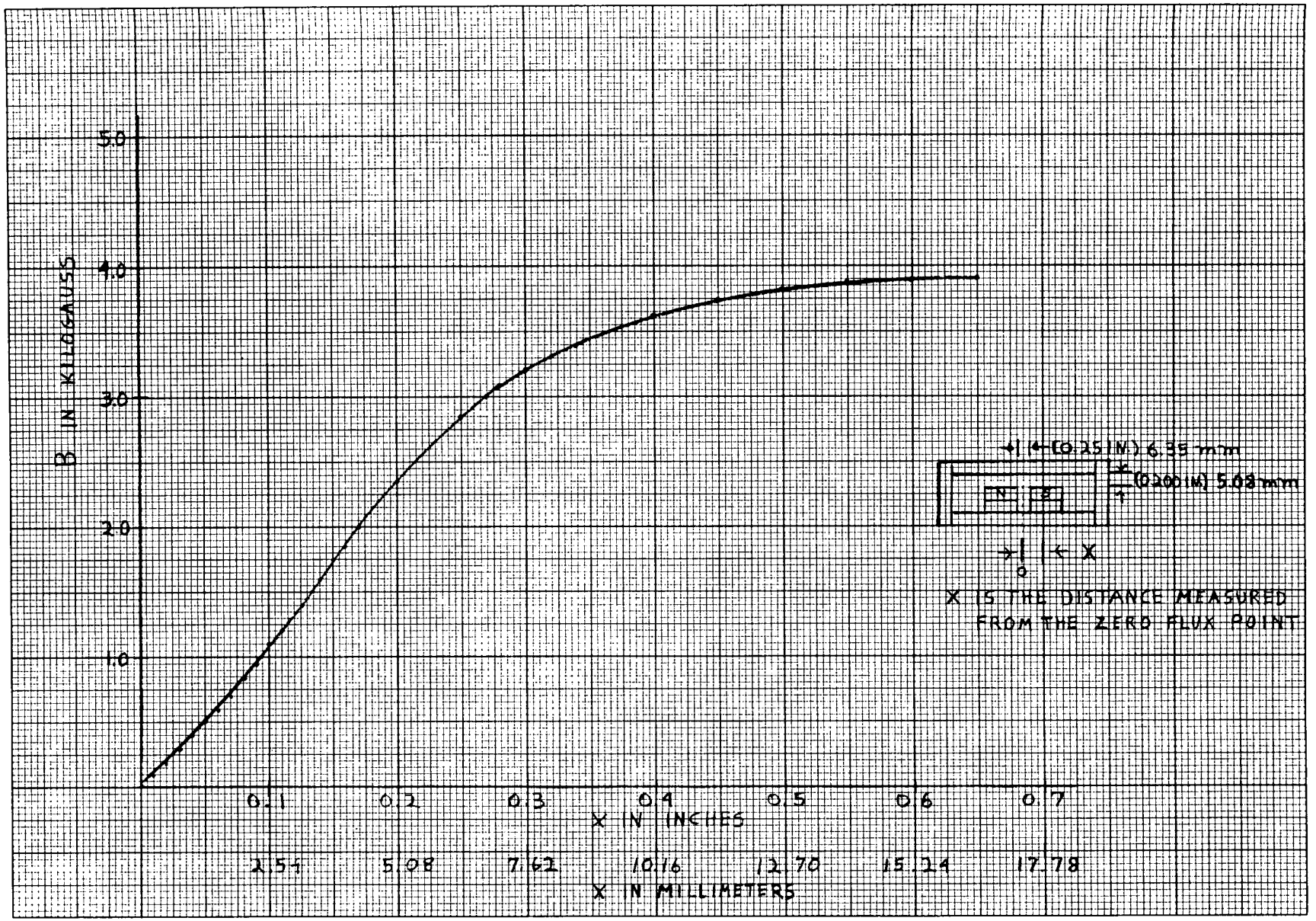

Figure 5-25. Flux Distribution With Magnets on One Side of Airgap

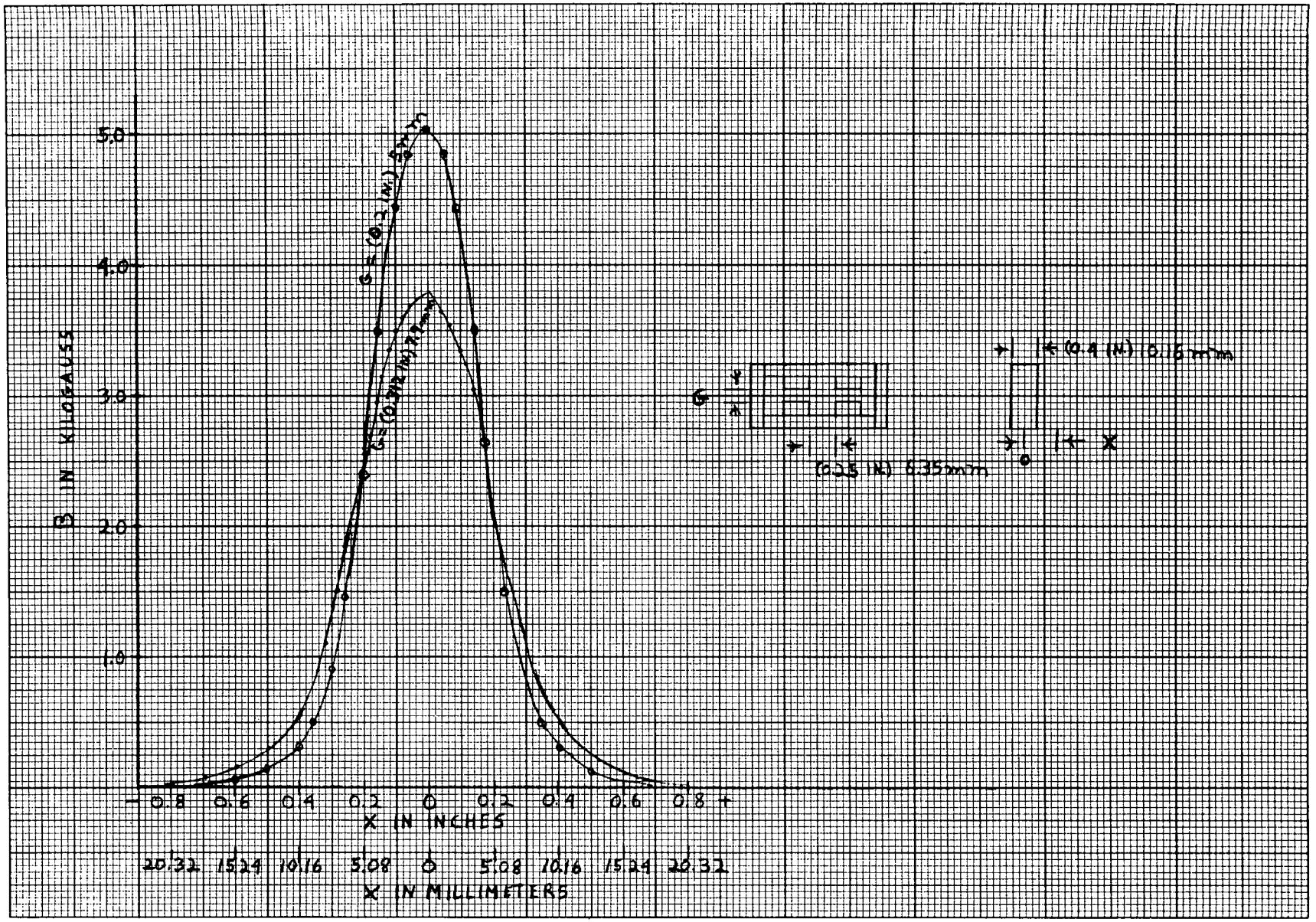

Figure 5-26. Flux Distribution in Axial Direction For Double Magnet Configuration

SECTION VI

RECOMMENDATIONS AND CONCLUSIONS

The ironless armature torque motor developed on NASA Contract NAS 5-11481 met or exceeded all specifications except for the generated voltage waveform. It is recommended that further effort be made to investigate the effect of coil shape on generated voltage waveform and to develop methods of improving the flux distribution.

The ironless armature torque motor is recommended for use in applications requiring low friction torques, low electrical time constants, or lack of decentering forces. High speed applications should be investigated.

Consideration should be given to making the outer magnetic ring, which is part of the rotor assembly, part of the stationary winding assembly. This would both reduce the overall weight due to the elimination of structural elements and provide a mechanically stronger stator assembly while adding very little magnetic friction.

SECTION VII

NEW TECHNOLOGY

Contractor by letter dated August 14, 1972 reported no inventions were made in the performance of work under this contract. Such report was made on DD Form 882 and copies forwarded to the Contracting Officer, Mr. P. Videniers. There were no discoveries, improvements or innovations made in performance of this contract other than reported in Contractor's Final Project Report JA 700-0020 dated September 10, 1972. The basic concept of the ironless armature torquer as applied to Brushless DC Motors is new technology. The use of samarium cobalt permanent magnets in the design of the ironless armature torquer is new technology in that this is one of the few motor applications that can effectively use this magnet material.

SECTION VIII

INDEX